

# Currency Network Risk

Mykola Babiak\*

*Lancaster University Management School*

Jozef Baruník\*\*

*Charles University*

First draft: December 2020

This draft: July 22, 2021

## Abstract

This paper identifies new currency risk stemming from a network of idiosyncratic option-based currency volatilities and shows how such network risk is priced in the cross-section of currency returns. A portfolio that buys net-receivers and sells net-transmitters of short-term linkages between currency volatilities generates a significant Sharpe ratio. The network strategy formed on causal connections is uncorrelated with popular benchmarks and generates a significant alpha, while network returns formed on aggregate connections, which are driven by a strong correlation component, are partially subsumed by standard factors. Long-term linkages are priced less, indicating a downward-sloping term structure of network risk.

**Keywords:** Foreign exchange rate, network risk, idiosyncratic volatility, currency predictability, term structure

**JEL:** G12, G15, F31

---

\*Department of Accounting & Finance, Lancaster University Management School, LA1 4YX, UK, E-mail: m.babiak@lancaster.ac.uk.

\*\*Institute of Economic Studies, Charles University, Opletalova 26, 110 00, Prague, CR and Institute of Information Theory and Automation, Academy of Sciences of the Czech Republic, Pod Vodarenskou Vezi 4, 18200, Prague, Czech Republic, E-mail: barunik@utia.cas.cz.

# 1 Introduction

Volatility has played a central role in economics and finance. In currency markets, a global volatility risk has been proposed by prior literature as a key driver of carry trade returns. While the global volatility risk factor is intuitively appealing, there is little evidence on how idiosyncratic currency volatilities relate to each other. This seems surprising since a shock to the ex-ante volatility of a particular currency possibly transmits to expectations about the future volatility of other currencies. These linkages consequently define weighted and directed network structures that contain information about transmission of idiosyncratic volatility shocks above and beyond fluctuations in global volatility. Since the connections are likely to be asymmetric, investors are unable to diversify away idiosyncratic shocks and, therefore, differences in the strength of directional volatility connections become important characteristics of currency risk. Guided by this insight and earlier evidence on network effects for firm-level stock volatilities (e.g., [Herskovic et al., 2020](#)), our goal is to understand currency volatility linkages and to test whether currency excess returns compensate for such network risk.

In this paper, we identify the dynamic network structure among idiosyncratic option-based currency volatilities. Using traded currency options, we measure how market fears stemming from uncertainty about future exchange rate fluctuations covary across currencies and how shocks to these fears create a network and spread within that network. The pure market-based approach we propose allows us to characterize the currency network risk on a daily basis as well as to use its forward-looking strength at the cost of minimal assumptions. We document two important sources of volatility linkages forming the networks – causal and correlation-based drivers. Exploring these networks, we show that the information contained in our networks is valuable for an investor.

The main contribution of the paper is that we present new empirical evidence regarding the behavior of currencies' idiosyncratic risk and examine the implications of this behavior for exchange rate predictability. First, ex-ante idiosyncratic volatilities of currencies form a connected network, which is driven by a strong correlation component as well as causal shocks between individual volatilities forming linkages. Second, both aggregate and causal network risks are priced in the cross-section of currency returns. Third, a portfolio

that buys net-receivers and sells net-transmitters of short-term linkages between currency volatilities generates a significant Sharpe ratio. The network strategy formed on causal linkages is uncorrelated with popular foreign exchange strategies and generates a significant alpha after controlling for the benchmarks. In contrast, network returns formed on aggregate connections, which are primarily driven by a strong correlation component, are partially subsumed by standard factors.

We begin our empirical investigation by constructing forward-looking measures of idiosyncratic volatilities of exchange rates. Specifically, we follow the model-free approach of [Britten-Jones and Neuberger \(2000\)](#) and [Bakshi et al. \(2003\)](#) to compute spot implied variances on exchange rates from currency option prices. The highly liquid and large foreign exchange volatility market provides an excellent opportunity to synthesize such measures.<sup>1</sup> Furthermore, the variance measures constructed from currency derivatives, which reflect the expectations of agents about future financial and real macroeconomic risks, are distinct from the backward-looking realized variance estimates.<sup>2</sup>

We continue by constructing novel forward-looking dynamic network of exchange rate volatilities. Our network measures are built in the tradition of dynamic predictive modeling under misspecification, and important causal linkages are approximated via time varying vector autoregression models ([Diebold and Yilmaz, 2014](#); [Barunik and Ellington, 2020](#)). The network of idiosyncratic volatilities inferred from time varying variance decompositions has several key attributes. First, the connections between volatilities of currencies are weighted and directed. That is, the influence of shocks to idiosyncratic volatilities are not symmetric in the system and such network then identifies information beyond standard correlation-based measures. Second, we are able to distinguish between short- and long-term connections among individual currency variances and hence we shed light on how a network risk stemming from shocks with different persistence is being priced in currency markets. Third, the international dependencies are naturally driven by contemporaneous fluctuations in global markets and causal influences. Our network measures allow to characterize such dependencies from forward-looking market data. In our empir-

---

<sup>1</sup>As of June 2019, daily average turnover was \$294 billion and notional amounts outstanding was \$12.7 trillion ([BIS, 2019a,b](#)). A wide variety of strikes and maturities available on the market allow us to precisely compute the implied variances on exchange rates.

<sup>2</sup>See, for example, [Gabaix and Maggiori \(2015\)](#), [Zviadadze \(2017\)](#), and [Colacito et al. \(2018\)](#) for the nature of risks traded in currency markets.

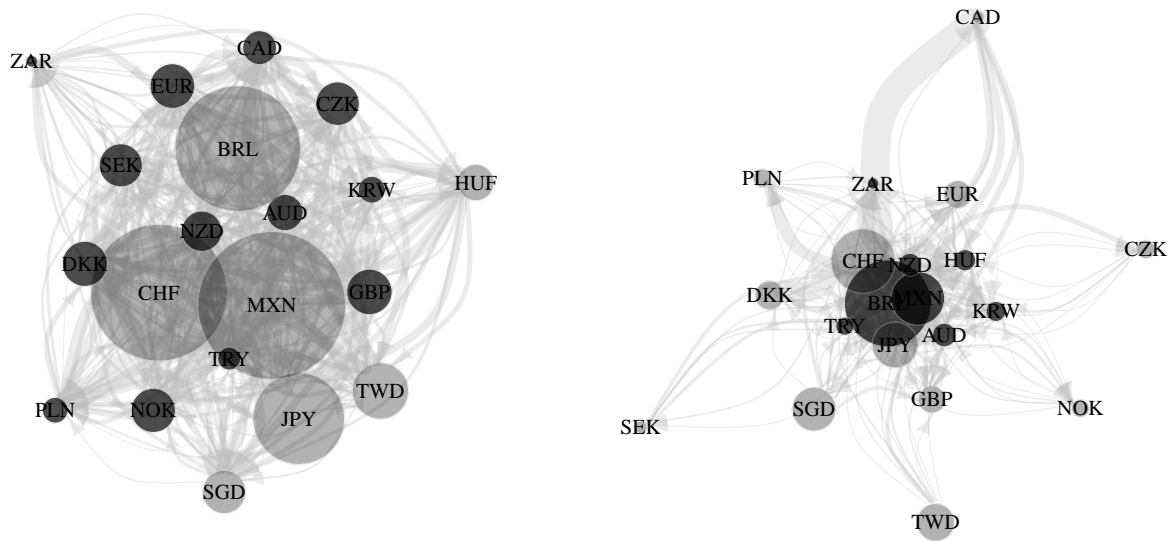


**Figure 1. Aggregate (left) and causal (right) short-term currency networks: September 30, 2008**

The left (right) figure depicts network connections among option-based currency variances based on aggregate (causal) connections of transitory nature. Aggregate network measures overall dependencies between currency variances, including correlation-based and causal effects. Causal network is obtained by removing contemporaneous correlations from aggregate network. Arrows denote the direction of connections and the strength of lines denotes the strength of linkages. Grey (black) vertices denote currencies receiving (transmitting) more shocks than transmitting (receiving) them. The size of vertices indicates the net-amount of shocks. To enhance readability of plots, links are drawn if intensities are above a predetermined threshold.

ical analysis, we are able to isolate causal linkages among currency variances by controlling for contemporaneous effects. Finally, the structure of volatility connections is changing dynamically over time, unlike the somewhat persistent relationships between countries based on interest rates. Hence, sorting currencies according to idiosyncratic volatility linkages is not equivalent, for example, to the currency carry trade.

To illustrate the above, Figure 1 depicts aggregate and causal short-term connections among currency volatilities of twenty developed and emerging market economies inferred from shocks of transitory nature. Figure 2 then demonstrates short- and long-term causal linkages based on both transitory and permanent shocks to volatilities. We can see that aggregate and causal connections convey significantly different structures of shock propagation between idiosyncratic volatilities. The contribution of shocks that carry transitory and permanent information creating short- and long-horizon network is changing dynam-

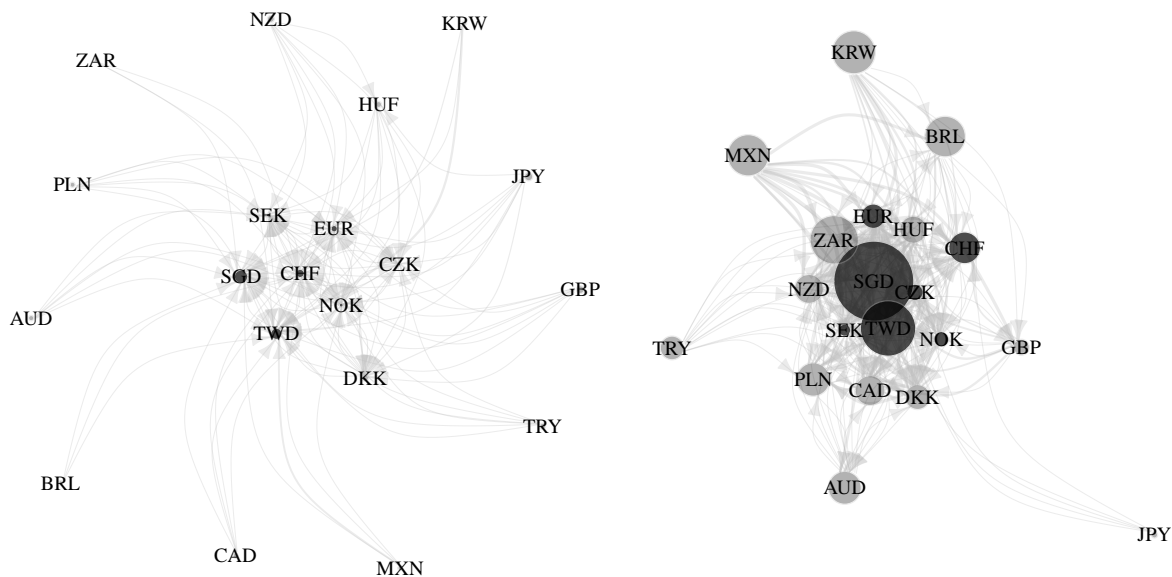


**Figure 2. Causal short-term (left) and long-term (right) currency networks: August 31, 2011**

The left (right) figure depicts short-term (long-term) network connections among option-based currency variances based on causal connections of transitory (permanent) nature of shocks. Causal connections are obtained by removing contemporaneous correlations from aggregate connections. Arrows denote the direction of connections and the strength of lines denotes the strength of linkages. Grey (black) vertices denote currencies receiving (transmitting) more shocks than transmitting (receiving). The size of vertices indicates the net-amount of shocks. To enhance readability of plots, links are drawn if intensities are above a pre-determined threshold.

ically. For example, shortly after the bankruptcy of Lehman Brothers, the market crashes were strongly driven by shocks to idiosyncratic volatility having transitory (short-term) impact, whereas fears of contagion in Europe reflect mainly permanent (long-term) risks. A natural question arises: what are the asset pricing implications of such structures in idiosyncratic volatility?

We document that network topology predicts currency returns. Empirically, we examine the profitability of strategies that buy net-receivers and sell net-transmitters of horizon-specific shocks in the network. For each currency volatility, we first compute the cumulative strength of transmitted/received connections and take the difference between them to obtain a net-directional connectedness. Further, we compute net-directional connectedness based on aggregate or causal linkages for short-, medium-, and long-term horizons.<sup>3</sup> We

<sup>3</sup>In the empirical investigation, we define short-term as a 1-day to 1-week horizon, medium-term as a 1-week to 1-month horizon, and long-term as a horizon longer than 1-month.

then build monthly quintile portfolios sorted by the net-directional network measures. For instance, for the short-term net-directional causal network, the first (fifth) portfolio contains the currencies transmitting (receiving) more short-term causal shocks than receiving (transmitting) them. We find that buying currencies of short-term net-receivers and selling currencies of short-term net-transmitters yields a high Sharpe ratio over the 1996-2013 period (0.65 and 0.80 for aggregate and causal connections). Regressing the excess returns of short-term net-directional portfolios on the dollar, carry trade, volatility, variance risk premium, and momentum strategies yields economically and statistically significant alphas, particularly for a causal network case (6.31% per annum with a t-stat of 3.48). To better understand the sources of this profitability, we sort the currencies into quintiles based on a combined strength of all transmitted (received) connections of idiosyncratic currency volatility to (from) others. The results show that this is the network risk related to transmitting shocks to others, which is strongly priced.

Relative to common currency portfolios, the predictability stemming from network risk is primarily driven by changes in exchange rates and not by interest rate differentials. The network strategies formed on causal linkages are also weakly correlated with currency benchmarks, providing excellent diversification gains. The allocation analysis demonstrates that the strategy using causal short-term net-directional connections buys or sells different currencies compared to benchmarks at least 40% of the time. In contrast, the excess returns of portfolios based on aggregate connections are driven strongly by interest differentials and are more correlated with other strategies. The results indicate a distinctive source of causal network returns.

We next focus on the term structure of network risk premiums. The risk-adjusted performance of network portfolios formed on net-directional connectedness decreases with the horizon of volatility linkages, suggesting that excess returns are related to transitory shocks. This is consistent with the downward-sloping term structure of unconditional forward risk premium in equity markets ([Dew-Becker et al., 2017](#)). Interestingly, average returns and Sharpe ratios of strategies formed on the amount of transmitted causal shocks slightly increase with the horizon.

Further, we examine whether excess returns of network-sorted portfolios reflect the

compensation for risk. For this purpose, we consider the cross-section of currency returns formed on the short-term net-directional connectedness computed for aggregate or causal connections. Following [Lustig et al. \(2011\)](#), we perform a principal component decomposition of test portfolios. The results show that the cross-section formed on aggregate linkages can be summarized by the first two principal components, whereas causal network portfolios require three components. Motivated by these results, we formally test a battery of two- and three-factor linear models. None of pricing kernels with benchmark factors can explain currency returns formed on aggregate or causal connectedness. In contrast, the corresponding network factor appears to be strongly priced. Finally, for the causal network cross-section, an augmented pricing kernel with the dollar, carry trade and causal net-directional network factors provides the best-performing three-factor model.

Our empirical evidence is robust to a number of robustness checks. First, the magnitude and significance of risk- and benchmark-adjusted returns of network portfolios increase monotonically when we move to weekly and daily frequencies. Second, the excess returns remain significant after adjusting them for transaction costs. Third, the network portfolios generate comparable performance statistics across the first and second half of the sample.

This paper contributes also to the literature documenting predictability in currency returns.<sup>4</sup> The volatility-related strategies exploit global foreign exchange volatility ([Menkhoff et al., 2012a](#)) and currency variance risk premium ([Della Corte et al., 2016](#)). [Gabaix and Maggiori \(2015\)](#) and [Colacito et al. \(2018\)](#) build the models explaining these strategies. We contribute to this literature by showing how network risk from option-based variances on exchange rates is priced in the cross-section of currency excess returns. Further, network returns stemming from the causal nature of linkages are virtually unrelated to the existing strategies. [Della Corte et al. \(2020\)](#) document a global risk factor in the cross-section of implied volatility returns. The key differentiator of our study from their work is that we study network risk of option-based currency variances in spot currency excess returns.

In related work, [Mueller et al. \(2017\)](#) propose a strategy based on the sensitivity of currencies to the cross-sectional dispersion of conditional foreign exchange correlation. They

---

<sup>4</sup>The literature proposes strategies, among others, based on the carry trade ([Lustig and Verdelhan, 2007](#); [Lustig et al., 2011](#); [Menkhoff et al., 2012a](#)), momentum ([Menkhoff et al., 2012b](#); [Asness et al., 2013](#); [Dahlquist and Hasseltoft, 2020](#)), business cycles ([Colacito et al., 2020](#)), and global imbalances ([Corte et al., 2016](#)).



construct the conditional correlation from spot exchange rates as well as using the currency options for the risk-neutral counterpart. They find some interesting results about the compensation for exposure to high or low dispersion states. In contrast, we focus on dependencies in currency variances instead of correlations of spot exchange rates. Furthermore, the connectedness measures of our paper are directional, unlike correlation-based proxies used by [Mueller et al. \(2017\)](#). Further, we are able to disentangle causal from contemporaneous effects in connections between currency variances.

Our paper is also related to [Richmond \(2019\)](#) who presents a model explaining the carry trade premium via the country’s position in the global trade network. Unlike network risk based on trade linkages, we study the market-based network from currency option-based variances. The currency excess returns sorted on network risk measures of our paper are weakly correlated to the standard carry trade. Hence, the predictive information of the network factor built from currency option prices is distinctive from trade links.

Finally, our paper is related to the literature focusing on downside risk in currency markets. [Jurek \(2014\)](#), [Burnside et al. \(2011\)](#), [Farhi et al. \(2015\)](#) and [Chernov et al. \(2018\)](#) investigate crash risk using currency options, while [Fan et al. \(2021\)](#) document an option-based equity tail factor in the cross-section of currency returns. Although we use option data to synthesize implied variances on exchange rates, our paper examines on the dependencies of idiosyncratic currency volatilities instead of downside risk.

## 2 Currency Network Risk

This section describes the construction of a network of idiosyncratic option-based currency variances and introduces currency network risk proxies studied in the core analysis.<sup>5</sup>

### 2.1 Currency Variance: Inferring Investor’s Expectations from Option Prices

We begin by synthesizing the risk-neutral expectation of exchange rate variances from quoted currency options. Specifically, we obtain spot implied variances from OTC currency options by applying a model-free approach of [Britten-Jones and Neuberger \(2000\)](#) and [Bakshi et al. \(2003\)](#). Formalizing the discussion, we use prices of European call and put options expiring at time  $t + \tau$  to compute the implied variance for an exchange rate  $k$

---

<sup>5</sup>Appendix A provides a detailed methodology used to estimate a dynamic horizon specific network.



versus the US dollar between two dates  $t$  and  $t + \tau$  :

$$\text{CIV}_{t,t+\tau}^k = \frac{2}{B^k(t,t+\tau)} \left\{ \int_{F^k(t,t+\tau)}^{\infty} \frac{C^k(t,t+\tau,K)}{K^2} dK + \int_0^{F^k(t,t+\tau)} \frac{P^k(t,t+\tau,K)}{K^2} dK \right\}, \quad (1)$$

where  $C^k(t,t+\tau,K)$  and  $P^k(t,t+\tau,K)$  denote the prices of call and put contracts at time  $t$  with a strike price  $K$  and maturity  $\tau$ ,  $B^k(t,t+\tau)$  is the price of a country's bond at time  $t$  with maturity  $\tau$ ,  $F^k(t,t+\tau)$  is the forward exchange rate of the currency  $k$  at time  $t$  with maturity  $\tau$ . To compute the model-free implied variances, we discretize the integral in Eq. (1) by adopting call and put option prices interpolated around the  $\tau$  maturity, and by considering a range of strike prices for the currency  $k$ .

## 2.2 Dynamic Network Risk

Having constructed forward-looking currency variances, our objective is to define the network for shocks of a specific persistence propagating across these variances. The knowledge of how an uncertainty shock to a currency  $j$  transmits to a currency  $k$  defines a directed link at a given period of time. These disaggregate connections between currency pairs then characterize two major types of network risk: a receiver or a transmitter of shocks. Aggregating the information from all pairs provides a system-wide measure of the forward-looking connectedness among foreign exchanges of countries. In contrast to the network literature in finance (Elliott et al., 2014; Glasserman and Young, 2016; Herkovic, 2018), we construct a highly dynamic network encompassing the information for a range of horizons into the future.

A dynamic network can be characterized well through variance decompositions from a time varying parameter vector autoregression (TVP-VAR) approximation model (Diebold and Yilmaz, 2014). Variance decompositions provide useful information about how much of the future variance of a variable  $j$  is due to shocks in a variable  $k$ . The time-varying variance decomposition matrix defines the dynamic network adjacency matrix and is intimately related to network node degrees, mean degrees, and connectedness measures. Further, a frequency domain view on such a network structure allows us to decompose the network to short-, medium- or long-term network risk (Diebold and Yilmaz, 2014).<sup>6</sup>

---

<sup>6</sup>A natural way to characterize horizon specific dynamics (i.e. short- and long-term) of the dynamic network risk is to consider the spectral representation of the approximating model as recently proposed by

Algebraically, the adjacency matrix captures all information about the network, and any sensible measure must be related to it. Network centrality is a typical metric used by the wide network literature, which provides the user with information about the relative importance or influence of nodes. For our purposes, we want to measure node degrees that capture the number of links to other nodes. The distribution shape of the node degrees is a network-wide property that closely relates to network behavior. As for the connectedness of the network, the location of the degree distribution is key, and hence, the mean of the degree distribution emerges as a benchmark measure of overall network connectedness.

The dynamic horizon specific networks we work with are more sophisticated than classical network structures. In a typical network, the adjacency matrix contains zero and one entries, depending respectively on the node being linked or not. In the above notion, one interprets variance decompositions as weighted links showing the strength of the connections. In addition, the links are directed, meaning that the  $j$  to  $k$  link is not necessarily the same as the  $k$  to  $j$  link, and hence, the adjacency matrix is not symmetric. These measures are the key to our analysis as directional connectedness risk stems directly from asymmetries within the network.

We construct a dynamic network through the TVP-VAR model estimated from currency implied variances following the methodology of [Barunik and Ellington \(2020\)](#). We consider a locally stationary TVP-VAR of a lag order  $p$  describing the dynamics as:

$$\mathbf{CIV}_{t,T} = \Phi_1(t/T)\mathbf{CIV}_{t-1,T} + \dots + \Phi_p(t/T)\mathbf{CIV}_{t-p,T} + \epsilon_{t,T}, \quad (2)$$

where  $\mathbf{CIV}_{t,T} = \left(\mathbf{CIV}_{t,T}^{(1)}, \dots, \mathbf{CIV}_{t,T}^{(N)}\right)^\top$  is a double indexed  $N$ -variate time series of currency variances,  $\epsilon_{t,T} = \Sigma^{-1/2}(t/T)\boldsymbol{\eta}_{t,T}$ ,  $\boldsymbol{\eta}_{t,T} \sim NID(0, \mathbf{I}_M)$  are normally distributed shocks,

$$\Phi(t/T) = (\Phi_1(t/T), \dots, \Phi_p(t/T))^\top$$

are the time varying autoregressive coefficients. Note that  $t$  refers to a discrete time index  $1 \leq t \leq T$  and  $T$  is an additional index indicating the sharpness of the local approximation of the time series by a stationary process. Rescaling time such that the continuous parameter  $u \approx t/T$  is a local approximation of the weakly stationary time-series ([Dahlhaus, 1996](#)), [Barunik and Ellington \(2020\)](#).

we approximate  $\mathbf{CIV}_{t,T}$  in a neighborhood of  $u_0 = t_0/T$  by a stationary process:

$$\widetilde{\mathbf{CIV}}_t(u_0) = \Phi_1(u_0)\widetilde{\mathbf{CIV}}_{t-1}(u_0) + \dots + \Phi_p(u_0)\widetilde{\mathbf{CIV}}_{t-p}(u_0) + \epsilon_t. \quad (3)$$

The TVP-VAR process has a time varying Vector Moving Average  $\text{VMA}(\infty)$  representation (Dahlhaus et al., 2009; Barunik and Ellington, 2020):

$$\mathbf{CIV}_{t,T} = \sum_{h=-\infty}^{\infty} \Psi_{t,T}(h)\epsilon_{t-h} \quad (4)$$

where a parameter vector  $\Psi_{t,T}(h) \approx \Psi(t/T, h)$  is a time varying impulse response function characterized by a bounded stochastic process.<sup>7</sup> Information contained in  $\Psi_{t,T}(h)$  permits the measurement of the contribution of shocks in the system. Hence, its transformations over time will determine the network risk. Since a shock to a variable in the model does not necessarily appear alone, an identification scheme is crucial in identifying the network. We adapt the extension of the generalized identification scheme of Pesaran and Shin (1998) to locally stationary process as proposed by Barunik and Ellington (2020).

We transform local impulse responses in the system to local impulse transfer functions using Fourier transformations. This allows us to measure the horizon specific dynamics of the network based on heterogeneous persistence of shocks in the system. A dynamic representation of the variance decomposition of shocks from a currency  $j$ 's variance to a currency  $k$ 's variance then establishes a dynamic horizon specific adjacency matrix, which is central to our network risk measures.

Specifically, the element of such a matrix, which captures how shocks from idiosyncratic variance of a currency  $j$  propagate to the variance of a currency  $k$  at a given point of time  $u = t_0/T$  and a given horizon  $d_i \in \mathcal{H} = \{S, M, L\}$ , is formally defined as:

$$\left[\theta(u, d_i)\right]_{j,k} = \frac{\widehat{\sigma}_{kk}^{-1} \sum_{\omega \in d_i} \left( \left[ \widehat{\Psi}(u, \omega) \widehat{\Sigma}(u) \right]_{j,k} \right)^2}{\sum_{\omega \in \mathcal{H}} \left[ \widehat{\Psi}(u, \omega) \widehat{\Sigma}(u) \widehat{\Psi}^\top(u, \omega) \right]_{j,j}}. \quad (5)$$

$\widehat{\Psi}(u, \omega) = \sum_{h=0}^{H-1} \sum_h \widehat{\Psi}(u, h) e^{-i\omega h}$  is an impulse transfer function estimated from Fourier

<sup>7</sup>Since  $\Psi_{t,T}(h)$  contains an infinite number of lags, we approximate the moving average coefficients at  $h = 1, \dots, H$  horizons.

frequencies  $\omega$  of impulse responses that cover a specific horizon  $d_i$ , which is one of short (S), medium (M), or long (L) horizons as defined for arbitrarily chosen bands of frequencies.<sup>8</sup> It is important to note that  $[\boldsymbol{\theta}(u, d)]_{j,k}$  is a natural disaggregation of traditional variance decompositions to a time-varying and  $h$ -horizon adjacency matrix. This is because the portion of the local error variance of the  $j$ -th variable at horizon  $h$  due to shocks in the  $k$ -th variable is scaled by the total variance of the  $j$ -th variable. As the rows of the dynamic adjacency matrix do not necessarily sum to one, we normalize the element in each by the corresponding row sum:  $[\tilde{\boldsymbol{\theta}}(u, d)]_{j,k} = [\boldsymbol{\theta}(u, d)]_{j,k} / \sum_{k=1}^N [\boldsymbol{\theta}(u, d)]_{j,k}$ . Eq. (5) defines a dynamic horizon specific network completely. Naturally, our adjacency matrix is filled with weighted links showing strengths of connections. The links are directional, meaning that the  $j$  to  $k$  link is not necessarily the same as the  $k$  to  $j$  link. In sum, the adjacency matrix is asymmetric, horizon specific and evolves dynamically.

To obtain the time-varying coefficient estimates  $\hat{\boldsymbol{\Phi}}_1(u), \dots, \hat{\boldsymbol{\Phi}}_p(u)$  and the time-varying covariance matrix  $\hat{\boldsymbol{\Sigma}}(u)$  at a given point of time  $u = t_0/T$ , we estimate the approximating model in Eq. (3) using Quasi-Bayesian Local-Likelihood (QBLL) methods (Petrova, 2019). Specifically, we use a kernel weighting function, which gives larger weights to those observations surrounding the period whose coefficient and covariance matrices are of interest. Using conjugate priors, the (quasi) posterior distribution of the parameters of the model are available analytically. This alleviates the need to use a Markov Chain Monte Carlo (MCMC) simulation algorithm and permits the use of parallel computing. We provide a detailed discussion of the estimation algorithm in Appendix A.

Finally, the variance decompositions of forecast errors from the VMA( $\infty$ ) representation require a truncation of the infinite horizon with a  $H$  horizon approximation. As  $H \rightarrow \infty$  the error disappears (Lütkepohl, 2005). We note here that  $H$  serves as an approximating factor and has no interpretation in the time-domain. We obtain horizon specific measures using Fourier transforms and set our truncation horizon  $H=100$ . The results are qualitatively similar for  $H \in \{50, 100, 200\}$ .

---

<sup>8</sup>Note that  $i = \sqrt{-1}$ .

### 2.3 Aggregate and Causal Effects: Removing Contemporaneous Correlations

An important feature we focus on is a direct causal interpretation of our network risk measures. [Rambachan and Shephard \(2019\)](#) provide a general discussion about causal interpretation of impulse response analysis in the time series literature. In particular, they argue that if an observable time series is shown to be a *potential outcome* time series, then generalized impulse response functions have a direct causal interpretation. Potential outcome series describe the output for a particular path of treatments at time  $t$ .

In the context of our study, paths of treatments are shocks. The assumptions required for a potential outcome series are natural and intuitive for a time series of currencies: i) they depend only on past and current shocks; ii) series are outcomes of shocks; and iii) assignments of shocks depend only on past outcomes and shocks. The dynamic adjacency matrix we use above to characterize the currency network risk is a transformation of generalized impulse response functions. Therefore, the adjacency matrix and all measures that stem from manipulations of its elements possess a causal interpretation; thus establishing the notion of causal dynamic network measures.

In computing our measures, we also diagonalize the covariance matrix because our objective is to focus on causal effects of network connections. The  $\Psi(u, d)$  matrix embeds the causal nature of network linkages, and the covariance matrix  $\Sigma(u)$  contains contemporaneous covariances within the off-diagonal elements. By diagonalizing the covariance matrix, we remove the contemporaneous effects and focus solely on causation. Hence, the measures introduced in the next section will be applied to aggregate and causal linkages depending on whether we include or exclude contemporaneous correlations.

### 2.4 Network Risk Measures

To evaluate network risk from the estimated model, we use several definitions that focus on disaggregate connections between currency variances. We introduce measures revealing when an individual currency is a transmitter or a receiver of uncertainty shocks.

First, horizon-specific from-directional network risk, which measures how much of each currency's  $j$  variance is due to shocks of other currencies' variances  $j \neq k$  in the cross-

section, is defined as:

$$\mathcal{F}_{j\leftarrow\bullet}(u, d) = \sum_{\substack{k=1 \\ k \neq j}}^N \left[ \tilde{\boldsymbol{\theta}}(u, d) \right]_{j,k} \quad d \in \{S, M, L\}. \quad (6)$$

Second, horizon-specific to-directional network risk, which measures the contribution of each currency's  $j$  variance to variances of other currencies in the cross-section, is given by:

$$\mathcal{T}_{j\rightarrow\bullet}(u, d) = \sum_{\substack{k=1 \\ k \neq j}}^N \left[ \tilde{\boldsymbol{\theta}}(u, d) \right]_{k,j} \quad d \in \{S, M, L\}. \quad (7)$$

One can interpret these measures as dynamic to-degrees and from-degrees that associate with the nodes of the weighted directed network captured by a variance decomposition matrix. The two measures show how other currencies contribute to the risk of a currency  $j$ , and how a currency  $j$  contributes to the riskiness of others in a time-varying fashion at a horizon  $d$ . Furthermore, from- and to-directional network risk measures are based on the network connections with a pre-specified persistence, which can be one of three choices: short- (S), medium- (M), or long-run (L). These horizons are determined by chosen bands of frequencies and aim to cover transitory, less persistent, and more persistent shocks. In the empirical analysis, we defined the short, medium, and long horizons as a 1-day to 1-week period, a 1-week to 1-month interval, and longer than 1-month, respectively. Adding these measures across all horizons defines a combined impact:

$$\mathcal{F}_{j\leftarrow\bullet}(u, T) = \sum_{d \in \{S, M, L\}} \mathcal{F}_{j\leftarrow\bullet}(u, d) \quad \wedge \quad \mathcal{T}_{j\rightarrow\bullet}(u, T) = \sum_{d \in \{S, M, L\}} \mathcal{T}_{j\rightarrow\bullet}(u, d) \quad (8)$$

Third, using two notions of receivers and transmitters of shocks presented above, we define a horizon specific net-directional network risk:

$$\mathcal{N}_{j\rightarrow\bullet}(u, d) = \mathcal{T}_{j\rightarrow\bullet}(u, d) - \mathcal{F}_{j\leftarrow\bullet}(u, d) \quad d \in \mathcal{H} = \{S, M, L, T\}. \quad (9)$$

Naturally, if the net-directional network measure is positive (negative) for a currency at time  $u$ , then we can interpret this currency as a net-transmitter (net-receiver) of shocks in the network.

In conclusion, we aim to study the properties of from-, to-, and net-directional network

portfolios sorted by corresponding network risk proxies defined by Eq. (6)-(9). Further, each portfolio group is constructed using aggregate and causal network linkages as discussed in Section 2.3.

### 3 Data and Currency Portfolios

#### 3.1 Currency Options Data

We start our empirical investigation by collecting daily OTC option implied volatilities on exchange rates versus the US dollar from JP Morgan and Bloomberg. Following [Della Corte et al. \(2016\)](#) and [Della Corte et al. \(2020\)](#), we consider a sample of the following 20 developed and emerging market countries: Australia, Brazil, Canada, the Czech Republic, Denmark, Euro Area, Hungary, Japan, Mexico, New Zealand, Norway, Poland, Singapore, South Africa, South Korea, Sweden, Switzerland, Taiwan, Turkey, and the United Kingdom. The data cover the sample period from January 1996 to December 2013. The cross-section begins with 10 currencies and gradually increases over time, with the data on all exchange rates being available from 2004 until the end of the sample in 2013.<sup>9</sup>

We synthesize spot implied variances using a model free approach of [Britten-Jones and Neuberger \(2000\)](#), which requires currency option prices for a range of strike prices. Quotes for OTC currency options are expressed in terms of [Garman and Kohlhagen \(1983\)](#) implied volatilities for selected combinations of plain-vanilla options (at-the-money, 10 and 25 delta put and call options). We recover strike prices from deltas and option prices from implied volatilities by employing interest rates from Bloomberg, spot and forward exchange rates from Barclays and Reuters via Datastream. Using this recovery procedure, we obtain plain vanilla European calls and puts for exchange rates versus the US dollar for a range of maturities: 1 month, 3 months, 6 months, 12 months, and 24 months.

Since our investment strategy is carried out at the monthly frequency, it is natural to assume that traders prefer to employ the 1-month spot implied variances on exchange rates for detecting network risk instead of using data for longer maturities. We therefore work with the spot 1-month variances on currencies in our empirical analysis. Further, we estimate the network using the variances at the daily frequency to increase the number of observations in our estimation procedure and ultimately to better capture the dynamic

---

<sup>9</sup>We greatly appreciate the help of Roman Kozhan with the currency option data.



nature of network risk. We then filter end-of-month estimates of how currencies are connected to each other to construct the long-short network portfolios.

### 3.2 Exchange Rate Data

We retrieve daily bid, mid, and ask spot and forward exchange rates versus the US dollar from Barclays and Reuters via Datastream. We further obtain daily nominal interest rates for domestic (the US in our case) and foreign countries from Bloomberg. The core empirical analysis is conducted at the monthly frequency and hence we sample end-of-month observations of all time series. We match exchange and interest rate data with currency option data for the cross-section of 20 countries and the sample period from January 1996 to December 2013 as described above.

### 3.3 Currency Excess Returns

We denote the spot and forward exchange rate of foreign currency  $k$  at time  $t$  as  $S_t^k$  and  $F_t^k$ . Exchange rates are expressed in units of foreign currency per US dollar. Thus, an increase in  $S_t^k$  indicates a depreciation of the foreign currency. Following [Menkhoff et al. \(2012a\)](#), we define one-period ahead excess return to a US investor for holding foreign currency  $k$  at time  $t$  as

$$rx_{t+1}^k = i_t^k - i_t - \Delta s_{t+1}^k \approx f_t^k - s_{t+1}^k, \quad (10)$$

in which  $i_t^k$  and  $i_t$  represent the risk-less rates of the foreign country  $k$  and the US,  $\Delta s_{t+1}^k$  is the log change in the spot exchange rate,  $f_t^k$  and  $s_{t+1}^k$  denote the log spot and forward rates. Under covered interest rate parity (CIP), the interest rate differential  $i_t^k - i_t$  is equal to forward discount  $f_t^k - s_t^k$ . Thus, the approximation in Eq. (10) states that the excess currency return equals the difference between the current forward rate and future spot rate. The early literature documented that CIP held even for very short horizons ([Akram et al., 2008](#)), while recent evidence has shown CIP deviations in the post global financial crisis period ([Du et al., 2018](#); [Andersen et al., 2019](#)). We demonstrate that the profitability of network strategies studied in our paper stems primarily from spot exchange rate predictability. Therefore, our key results do not depend on the validity of the CIP condition.

### 3.4 Network Portfolios

The network measures introduced in Section 2.4 capture multiple risks that could be important for investors forming currency portfolios. First, unlike the previous literature

focusing on the correlation risk in currency returns, the network risk proxies of our paper can identify the causal nature of linkages by removing contemporaneous effects. Thus, we are able to detect novel risks originating from the causal propagation of shocks in the network of exchange rate variances. Second, using individual connections between exchange rates, we can quantify the aggregate amount of shocks that a particular currency transmits to or receives from others. Similarly, we can compute the net-directional connectedness measure by taking the difference between shocks that are transmitted and received. Third, a large strand of the literature studies the role of shocks with different persistences. For instance, long-term fluctuations in expected growth and volatility of cash-flows (Bansal and Yaron, 2004) have played a central role for understanding equity, bond, and currency returns. Our econometric methodology allows us to disentangle the effect of horizon specific linkages. We can therefore shed light on the term structure of network risk. In sum, we construct a battery of portfolios based on a variety of network measures to quantitatively evaluate which network risks are priced in currency markets.

At the end of each time period  $t$  (the last day of the month), we sort currencies into five portfolios using one of network measures constructed and described in Section 2.4. The first quintile portfolio  $\mathcal{P}_1$  comprises 20% of all currencies with the highest values of a particular network characteristic, whereas the fifth quintile portfolio  $\mathcal{P}_5$  contains 20% of all currencies with the lowest values. Each  $\mathcal{P}_i$  is an equally weighted portfolio of the corresponding currencies. We next form a long-short strategy that buys  $\mathcal{P}_5$  and sells  $\mathcal{P}_1$ .

We report the results for five quintile portfolios and a long-short strategy sorted by (i) short- (S), medium- (M), and long-term (L) as well as total (T) net-directional connectedness constructed from aggregate (contemporaneous and causal) and only causal linkages. The corresponding zero-cost strategies are denoted by  $\mathcal{N}(\mathcal{H})$  in which  $\mathcal{H} \in \{S, M, L, T\}$ . We additionally dissect the sources of profitability of net-directional network strategies by solely looking at the risk of being a transmitter or a receiver of shocks. In particular, we construct the portfolios based on (ii) to-directional and (iii) from-directional connectedness measures. Similarly to the portfolios in (i), we report the results for all horizons considered, but for the sake of a convenient illustration we focus on the case with causal linkages.<sup>10</sup> The

---

<sup>10</sup>The results of quintile and zero-cost portfolios sorted on to- and from-directional connections with aggregate linkages are available upon request.

respective to-directional and from-directional long-short portfolios are denoted by  $\mathcal{T}(\mathcal{H})$  and  $\mathcal{F}(\mathcal{H})$  in which  $\mathcal{H} \in \{S, M, L, T\}$ .

### 3.5 Dollar and Carry Trade Strategies

We compare the performance of network-sorted portfolios to standard strategies from the existing literature. Following [Lustig et al. \(2011\)](#), we build a portfolio that is the average of all currencies available in a particular time period. The resulting returns are equivalent to borrowing money in the US and investing in global money markets outside the US. This strategy is commonly called the dollar risk factor or the dollar portfolio (dol). Further, we sort all currencies available at time  $t$  into five quintile portfolios on the basis of their interest rate differential (or forward premia) relative to the US. The first quintile portfolio  $\mathcal{P}_1$  comprises 20% of all currencies with the highest interest rates, whereas the fifth quintile portfolio  $\mathcal{P}_5$  contains 20% of all currencies with the lowest interest rates. The difference between  $\mathcal{P}_1$  and  $\mathcal{P}_5$  is called the carry trade strategy (car), which is equivalent to borrowing money in low interest rate countries and investing in high interest rate countries.

### 3.6 Volatility Portfolios

We create a tradable strategy taking into account past realized volatility of currencies in the spirit of [Menkhoff et al. \(2012a\)](#). At the end of each month  $t$ , we compute the square root of the sum of squared daily log exchange rate returns during the current month. We sort all currencies available at time  $t$  into five quintile portfolios on the basis of their monthly realized volatility. The first quintile portfolio  $\mathcal{P}_1$  comprises 20% of all currencies with the highest volatility, whereas the fifth quintile portfolio  $\mathcal{P}_5$  contains 20% of all currencies with the lowest volatility. The difference between  $\mathcal{P}_1$  and  $\mathcal{P}_5$  is called the volatility strategy (vol), which is equivalent to selling currencies of low volatility risk countries and buying those of high volatility risk countries.

### 3.7 Variance Risk Premium Portfolios

We construct an investment strategy reflecting the costs of insuring currency variance risk that was recently proposed by [Della Corte et al. \(2016\)](#). At the end of each month  $t$ , we compute the volatility risk premium (vrp) for each currency, that is, the difference between

expected realized volatility and implied volatility over the next month.<sup>11</sup> We sort all currencies available at time  $t$  into five quintile portfolios on the basis of their monthly vrp. The first quintile portfolio  $\mathcal{P}_1$  comprises 20% of all currencies with the highest vrp, whereas the fifth quintile portfolio  $\mathcal{P}_5$  contains 20% of all currencies with the lowest vrp. The difference between  $\mathcal{P}_1$  and  $\mathcal{P}_5$  is called the volatility risk premia strategy, which is equivalent to selling high-insurance-cost currencies and buying low-insurance-cost currencies.

### 3.8 Momentum Portfolios

We form a tradable strategy linked to the past performance of currencies as initially proposed by [Menkhoff et al. \(2012b\)](#). Recently, [Dahlquist and Hasseltoft \(2020\)](#) further connect currency returns to past trends in fundamentals including economic activity and inflation. At the end of each month  $t$ , we compute the average of currency excess returns over the last six months.<sup>12</sup> We sort all currencies available at time  $t$  into five quintile portfolios on the basis of their trend. The first quintile portfolio  $\mathcal{P}_1$  comprises 20% of all currencies with the highest average returns, whereas the fifth quintile portfolio  $\mathcal{P}_5$  contains 20% of all currencies with the lowest average returns. The difference between  $\mathcal{P}_1$  and  $\mathcal{P}_5$  is called the momentum strategy (mom), which is equivalent to selling past losers (or worst performing currencies) and buying past winners (or best performing currencies).

## 4 Network Risk and Currency Returns

### 4.1 Net-directional Connectedness

Table 1 reports summary statistics of excess returns of five quintile portfolios ( $\mathcal{P}_i : i = 1, \dots, 5$ ) and the long-short investment strategy buying  $\mathcal{P}_5$  and selling  $\mathcal{P}_1$ . Further, Panels A and B present the results for a horizon specific net-directional portfolios formed on aggregate and causal connections. Several observations from Table 1 are noteworthy.

First, the average returns of  $\mathcal{N}(S)$  portfolios are 5.53% and 6.43% per annum for aggregate and causal linkages, which are statistically different from zero at the 5% and 1% levels, respectively. The “fx (%)” and “ir (%)” rows further indicate that this predictability stemming from aggregate connections is partially driven by predicting the interest rate

<sup>11</sup>[Della Corte et al. \(2016\)](#) work with the one-year volatility risk premium. We decide to switch to the monthly horizon to ensure that the volatility risk premium strategy employs one-month implied volatilities on exchange rates consistent with network portfolios.

<sup>12</sup>Our results remain quantitatively similar for other lags over which the past performance is evaluated.

differential. This result is expected in light of the prior literature ([Menkhoff et al., 2012a](#)) documenting a link between global foreign exchange volatility, which is strongly reflected in contemporaneous covariances of network linkages, and the carry trade strategy, which is entirely driven by the forward premium across countries. In contrast, the spread between  $\mathcal{P}_5$  and  $\mathcal{P}_1$  portfolios, which are constructed from the causal nature of network linkages, is largely driven by predicting the spot exchange rates. For instance, Panel B shows that the spread in the exchange rate component of excess returns of  $\mathcal{N}(S)$  is almost twice-as-large compared to that reported in Panel A (4.33% versus 2.28% per annum), whereas the spread in the interest rate differential substantially shrinks from 3.24% to 2.10% per annum. Also, there is no monotonicity in the forward premium as we move from  $\mathcal{P}_1$  to  $\mathcal{P}_5$  portfolios.

Second, the risk-adjusted performance of long-short portfolios deteriorates with the horizon of net-directional network risk. Using aggregate linkages, the annualized Sharpe ratio of network strategies gradually declines from 0.65 to 0.50 and 0.32 when using medium- and long- instead of short-term connections. The causal network portfolios experience a steeper decline in the annualized Sharpe ratio, from 0.80 to 0.47 and 0.39 when moving from short- to medium- and long-term horizons. Interestingly, the  $\mathcal{N}(T)$  portfolio based on causal linkages exhibits the annualized Sharpe ratio of 0.66 and the average return of 4.90% per annum, which is statistically different from zero at the 1% level. Overall, the results indicate the downward-sloping term structure of network risk in the cross-section of currency returns. This result extends the findings of the existing literature on the price of variance risk in equity markets ([Dew-Becker et al., 2017](#)).

Third, the excess returns of the best-performing network portfolio exploiting causal short-term linkages exhibit a low standard deviation, a positive skew, and a sizeable kurtosis. The volatility statistic implies that the improved Sharpe ratio originates not only from higher returns but also from their moderate time-variation. According to the skewness and kurtosis statistics, the portfolio formed on short-term causal connections is the only specification that tends to experience gains rather than losses and to have with more outliers in the right tail of the distribution. Indeed, analyzing the strategy's best and worst months, the portfolio experiences the three highest monthly returns of 7.98% in September 2002, 8.49% in August 1998, and 13.07% in October 2008, and the three lowest monthly returns of -4.61% in July 2002, -4.66% in August 2002, and -4.85% in January 1998. In con-

**Table 1. Net-directional Network Portfolios**

This table presents descriptive statistics for quintile ( $\mathcal{P}_i : i = 1, \dots, 5$ ) and long-short portfolios ( $\mathcal{N}(\cdot)$ ) sorted by short- ( $S$ ), medium- ( $M$ ), and long-term ( $L$ ) as well as total ( $T$ ) net-directional connectedness extracted from aggregate (Panel A) and causal (Panel B) linkages. The portfolio  $\mathcal{P}_1(\mathcal{P}_5)$  comprises currencies with the highest (lowest) network characteristic. The long-short portfolio buys  $\mathcal{P}_5$  and sells  $\mathcal{P}_1$ . Mean, standard deviation, and Sharpe ratio are annualized, but t-statistic of mean, skewness, kurtosis and the first-order autocorrelation are based on monthly returns. We also report the annualized mean of exchange rate ( $fx = -\Delta s^k$ ) and interest rate ( $ir = i^k - i$ ) components of excess returns. The t-statistics are based on [Newey and West \(1987\)](#) standard errors with [Andrews \(1991\)](#) optimal lag selection. The sample is from January 1996 to December 2013.

Panel A: Aggregate linkages												
	$\mathcal{P}_1$	$\mathcal{P}_2$	$\mathcal{P}_3$	$\mathcal{P}_4$	$\mathcal{P}_5$	$\mathcal{N}(S)$	$\mathcal{P}_1$	$\mathcal{P}_2$	$\mathcal{P}_3$	$\mathcal{P}_4$	$\mathcal{P}_5$	$\mathcal{N}(M)$
mean (%)	-0.69	0.35	1.65	1.44	4.84	5.53	-0.78	1.67	2.09	1.35	3.38	4.16
t-stat	-0.26	0.13	0.70	0.65	2.27	2.46	-0.30	0.63	0.87	0.68	1.34	1.83
fx (%)	-1.03	-0.45	-0.37	-1.30	1.26	2.28	-0.97	0.94	0.46	-1.44	-0.72	0.24
ir (%)	0.34	0.81	2.03	2.75	3.58	3.24	0.18	0.73	1.63	2.79	4.10	3.92
net	0.13	0.08	0.01	-0.06	-0.14	-0.27	0.07	0.05	0.00	-0.04	-0.08	-0.15
Sharpe	-0.06	0.03	0.18	0.16	0.61	0.65	-0.08	0.16	0.22	0.16	0.39	0.50
std (%)	10.70	10.48	9.36	8.80	7.91	8.52	10.35	10.30	9.34	8.70	8.76	8.29
skew	-0.15	-0.91	-0.48	-0.29	-0.13	-0.39	-0.22	-0.79	-0.13	-0.34	-1.34	-0.40
kurt	3.95	6.43	5.48	4.69	4.17	4.26	3.61	5.86	4.68	4.01	8.84	4.58
ac1	0.06	0.08	0.05	-0.04	0.13	0.10	0.02	0.05	0.06	-0.06	0.26	0.20
	$\mathcal{P}_1$	$\mathcal{P}_2$	$\mathcal{P}_3$	$\mathcal{P}_4$	$\mathcal{P}_5$	$\mathcal{N}(L)$	$\mathcal{P}_1$	$\mathcal{P}_2$	$\mathcal{P}_3$	$\mathcal{P}_4$	$\mathcal{P}_5$	$\mathcal{N}(T)$
mean (%)	0.05	0.41	2.54	1.94	2.81	2.76	-0.40	0.61	2.12	0.99	3.94	4.34
t-stat	0.02	0.15	1.01	0.85	1.33	1.20	-0.15	0.23	0.88	0.43	1.84	1.91
fx (%)	-0.16	-0.31	0.72	-0.79	-1.15	-0.99	-0.63	-0.03	0.28	-1.66	-0.10	0.53
ir (%)	0.22	0.72	1.82	2.73	3.96	3.74	0.23	0.64	1.84	2.65	4.04	3.81
net	0.05	0.03	0.00	-0.02	-0.05	-0.10	0.25	0.15	0.00	-0.13	-0.26	-0.52
Sharpe	0.01	0.04	0.26	0.22	0.33	0.32	-0.04	0.06	0.23	0.11	0.50	0.51
std (%)	10.51	9.83	9.86	8.72	8.42	8.70	10.68	10.06	9.16	9.40	7.81	8.43
skew	-0.46	-0.66	-0.15	-0.59	-0.65	0.01	-0.41	-0.48	-0.66	-0.45	-0.54	-0.29
kurt	4.77	5.15	4.87	6.21	4.82	5.12	4.95	4.23	5.67	4.46	4.01	4.13
ac1	0.04	0.13	0.03	0.03	0.08	0.09	0.04	0.07	0.04	0.02	0.16	0.12
Panel B: Causal linkages												
	$\mathcal{P}_1$	$\mathcal{P}_2$	$\mathcal{P}_3$	$\mathcal{P}_4$	$\mathcal{P}_5$	$\mathcal{N}(S)$	$\mathcal{P}_1$	$\mathcal{P}_2$	$\mathcal{P}_3$	$\mathcal{P}_4$	$\mathcal{P}_5$	$\mathcal{N}(M)$
mean (%)	-0.12	0.76	1.12	-0.18	6.31	6.43	-0.46	3.17	1.20	1.26	2.95	3.42
t-stat	-0.05	0.28	0.47	-0.07	3.11	3.81	-0.20	1.36	0.52	0.53	1.22	2.10
fx (%)	-2.14	-0.09	0.27	-1.68	2.20	4.33	-2.49	2.18	-0.27	-0.58	-0.10	2.39
ir (%)	2.01	0.84	0.84	1.50	4.11	2.10	2.03	0.99	1.47	1.84	3.05	1.02
net	0.03	0.00	-0.01	-0.01	-0.02	-0.05	0.03	-0.01	-0.01	-0.02	-0.03	-0.06
Sharpe	-0.01	0.08	0.12	-0.02	0.82	0.80	-0.05	0.36	0.13	0.13	0.32	0.47
std (%)	9.88	9.91	9.36	9.55	7.73	8.08	9.40	8.91	9.21	9.33	9.34	7.21
skew	-0.72	-0.90	-0.59	-0.22	-0.50	0.95	-0.87	-0.07	-0.54	-0.47	-0.63	0.07
kurt	5.32	5.62	5.63	4.72	4.07	6.86	5.79	3.68	4.43	4.99	5.61	3.46
ac1	-0.04	0.08	0.06	0.07	0.08	-0.15	0.01	0.05	0.02	0.06	0.10	-0.04
	$\mathcal{P}_1$	$\mathcal{P}_2$	$\mathcal{P}_3$	$\mathcal{P}_4$	$\mathcal{P}_5$	$\mathcal{N}(L)$	$\mathcal{P}_1$	$\mathcal{P}_2$	$\mathcal{P}_3$	$\mathcal{P}_4$	$\mathcal{P}_5$	$\mathcal{N}(T)$
mean (%)	-0.20	3.36	1.33	0.96	2.53	2.73	-0.26	2.11	1.04	0.33	4.64	4.90
t-stat	-0.09	1.36	0.55	0.41	1.05	1.83	-0.11	0.88	0.41	0.13	2.14	3.03
fx (%)	-2.20	1.98	-0.19	-0.69	-0.40	1.81	-2.27	1.26	-0.29	-1.33	1.12	3.39
ir (%)	2.00	1.38	1.52	1.65	2.92	0.93	2.01	0.84	1.33	1.65	3.52	1.51
net	0.03	0.00	-0.01	-0.02	-0.03	-0.06	0.10	-0.02	-0.04	-0.05	-0.08	-0.18
Sharpe	-0.02	0.36	0.14	0.11	0.26	0.39	-0.03	0.23	0.11	0.03	0.52	0.66
std (%)	9.16	9.36	9.50	8.88	9.64	7.07	9.47	9.08	9.67	9.44	8.89	7.44
skew	-0.77	-0.28	-0.43	-0.68	-0.50	0.01	-0.69	-0.27	-0.68	-0.36	-0.76	-0.32
kurt	5.56	3.51	4.07	5.30	5.27	3.47	5.17	3.77	5.27	4.66	5.89	4.94
ac1	0.00	0.05	0.04	0.09	0.05	-0.05	-0.02	0.03	0.04	0.16	0.05	-0.03

**Table 2. To- and From-directional Network Portfolios: Causal Linkages**

This table presents descriptive statistics for quintile ( $\mathcal{P}_i : i = 1, \dots, 5$ ) and long-short portfolios ( $\mathcal{T}(\cdot)$  and  $\mathcal{F}(\cdot)$ ) sorted by short- ( $S$ ), medium- ( $M$ ), and long-term ( $L$ ) as well as total ( $T$ ) to-directional (Panel A) and from-directional (Panel B) connectedness extracted from causal linkages. The portfolio  $\mathcal{P}_1$  ( $\mathcal{P}_5$ ) comprises currencies with the highest (lowest) network characteristic. The long-short portfolio buys  $\mathcal{P}_5$  and sells  $\mathcal{P}_1$ . Mean, standard deviation, and Sharpe ratio are annualized, but t-statistic of mean, skewness, kurtosis and the first-order autocorrelation are based on monthly returns. We also report the average network characteristic (net), the annualized mean of exchange rate ( $fx = -\Delta s^k$ ) and interest rate ( $ir = i^k - i$ ) components of excess returns. The t-statistics are based on [Newey and West \(1987\)](#) standard errors with [Andrews \(1991\)](#) optimal lag selection. The sample is from January 1996 to December 2013.

Panel A: To-directional network portfolios												
	$\mathcal{P}_1$	$\mathcal{P}_2$	$\mathcal{P}_3$	$\mathcal{P}_4$	$\mathcal{P}_5$	$\mathcal{T}(S)$	$\mathcal{P}_1$	$\mathcal{P}_2$	$\mathcal{P}_3$	$\mathcal{P}_4$	$\mathcal{P}_5$	$\mathcal{T}(M)$
mean (%)	0.04	0.00	-0.04	1.47	6.14	6.10	-0.61	0.92	0.16	1.54	5.91	6.52
t-stat	0.02	0.00	-0.02	0.66	3.13	3.66	-0.26	0.34	0.06	0.70	2.88	3.67
fx (%)	-1.92	-0.78	-0.89	-0.22	2.10	4.01	-2.52	-0.08	-0.63	-0.06	1.85	4.37
ir (%)	1.96	0.79	0.85	1.68	4.05	2.09	1.91	0.99	0.79	1.60	4.06	2.15
net	1.13	1.05	1.04	1.03	1.01	-0.12	1.37	1.18	1.13	1.09	1.05	-0.31
Sharpe	0.00	0.00	0.00	0.16	0.82	0.74	-0.06	0.09	0.02	0.18	0.77	0.80
std (%)	9.79	10.11	10.32	8.88	7.47	8.27	9.96	10.24	9.71	8.76	7.64	8.13
skew	-0.53	-0.83	-0.80	-0.47	-0.46	0.36	-0.61	-0.80	-0.71	-0.20	-0.40	0.24
kurt	4.45	6.26	5.75	4.94	4.15	5.30	4.40	5.78	5.78	4.09	4.01	4.00
ac1	-0.08	0.12	0.07	0.07	0.05	-0.15	-0.05	0.09	0.02	0.08	0.09	-0.11
	$\mathcal{P}_1$	$\mathcal{P}_2$	$\mathcal{P}_3$	$\mathcal{P}_4$	$\mathcal{P}_5$	$\mathcal{T}(L)$	$\mathcal{P}_1$	$\mathcal{P}_2$	$\mathcal{P}_3$	$\mathcal{P}_4$	$\mathcal{P}_5$	$\mathcal{T}(T)$
mean (%)	-0.48	0.64	0.38	1.25	6.13	6.61	-0.36	0.38	1.01	1.15	5.63	5.99
t-stat	-0.20	0.25	0.15	0.55	2.96	3.99	-0.15	0.14	0.39	0.55	2.74	3.49
fx (%)	-2.37	-0.18	-0.61	-0.25	1.97	4.35	-2.32	-0.59	0.20	-0.38	1.57	3.89
ir (%)	1.89	0.82	0.99	1.50	4.16	2.26	1.96	0.97	0.81	1.53	4.06	2.10
net	1.60	1.32	1.25	1.18	1.11	-0.49	1.27	1.12	1.09	1.06	1.03	-0.24
Sharpe	-0.05	0.06	0.04	0.14	0.80	0.83	-0.04	0.04	0.10	0.13	0.73	0.74
std (%)	9.65	10.27	9.83	9.06	7.69	7.99	10.02	9.98	9.94	8.66	7.66	8.05
skew	-0.48	-0.53	-0.56	-0.64	-0.41	0.26	-0.74	-0.63	-0.93	-0.26	-0.39	0.33
kurt	3.99	4.24	5.62	5.12	4.03	4.09	5.08	5.10	6.47	4.33	4.01	4.29
ac1	-0.02	0.04	0.01	0.10	0.07	-0.19	-0.05	0.10	0.05	0.04	0.09	-0.13
Panel B: From-directional network portfolios												
	$\mathcal{P}_1$	$\mathcal{P}_2$	$\mathcal{P}_3$	$\mathcal{P}_4$	$\mathcal{P}_5$	$\mathcal{F}(S)$	$\mathcal{P}_1$	$\mathcal{P}_2$	$\mathcal{P}_3$	$\mathcal{P}_4$	$\mathcal{P}_5$	$\mathcal{F}(M)$
mean (%)	0.85	1.97	1.85	1.49	1.51	0.67	0.57	1.47	1.86	2.41	1.98	1.41
t-stat	0.33	0.75	0.77	0.71	0.72	0.43	0.21	0.56	0.86	1.13	0.92	0.85
fx (%)	-1.51	0.25	0.29	-0.26	-0.62	0.89	-1.19	0.22	0.19	0.44	-0.86	0.33
ir (%)	2.36	1.72	1.56	1.75	2.14	-0.22	1.76	1.25	1.67	1.97	2.84	1.08
net	1.07	1.06	1.05	1.05	1.05	-0.02	1.39	1.29	1.24	1.19	1.13	-0.26
Sharpe	0.08	0.21	0.19	0.17	0.18	0.09	0.05	0.15	0.21	0.27	0.25	0.19
std (%)	10.76	9.54	9.51	8.68	8.30	7.26	10.68	9.85	9.04	8.88	7.96	7.58
skew	-0.50	-0.87	-0.46	0.02	-0.64	0.02	-0.59	-0.73	-0.28	-0.69	-0.11	-0.03
kurt	4.23	5.24	5.73	3.30	4.78	3.63	4.99	5.23	4.12	5.07	3.31	3.90
ac1	-0.01	0.20	0.02	-0.04	0.06	-0.11	0.04	0.09	0.06	0.01	0.07	-0.03
	$\mathcal{P}_1$	$\mathcal{P}_2$	$\mathcal{P}_3$	$\mathcal{P}_4$	$\mathcal{P}_5$	$\mathcal{F}(L)$	$\mathcal{P}_1$	$\mathcal{P}_2$	$\mathcal{P}_3$	$\mathcal{P}_4$	$\mathcal{P}_5$	$\mathcal{F}(T)$
mean (%)	1.48	1.19	0.98	2.46	2.07	0.59	-0.37	2.93	2.42	1.11	2.15	2.52
t-stat	0.58	0.46	0.40	1.11	0.98	0.36	-0.14	1.15	1.14	0.49	1.00	1.59
fx (%)	-0.29	-0.04	-0.62	0.41	-0.77	-0.48	-2.28	1.58	0.69	-0.92	-0.36	1.92
ir (%)	1.77	1.22	1.60	2.05	2.84	1.07	1.91	1.35	1.74	2.04	2.51	0.60
net	2.05	1.74	1.57	1.41	1.23	-0.83	1.24	1.19	1.16	1.13	1.09	-0.15
Sharpe	0.15	0.12	0.11	0.27	0.25	0.08	-0.04	0.29	0.28	0.12	0.27	0.34
std (%)	10.11	9.97	9.25	9.11	8.36	7.22	10.54	10.24	8.67	9.09	8.02	7.40
skew	-0.38	-0.58	-0.87	0.03	-0.30	0.01	-0.44	-0.92	-0.30	-0.56	-0.20	-0.31
kurt	4.37	5.19	6.00	4.24	4.42	3.20	4.54	6.21	4.79	4.53	3.20	4.26
ac1	0.04	0.07	0.09	0.03	0.02	-0.06	0.02	0.04	0.04	0.03	0.08	-0.04



trast, the excess returns of the network portfolio based on aggregate short-term linkages has a negative skewness, smaller maximal growth rates (6.10% in February 1997, 6.23% in October 1998, and 7.17% in May 2005) and deeper crashes (-6.18% in June 2002, -6.20% in December 2000, and -10.02% in December 2008).

#### 4.2 To- and From-directional Connectedness

Table 2 presents the performance statistics of the excess returns sorted on to-directional (Panel A) and from-directional (Panel B) connectedness extracted from causal linkages. The table shows the results for horizon-specific network risk measures.

For the to-directional case, the spread between the excess returns of  $\mathcal{P}_5$  and  $\mathcal{P}_1$  portfolios is increasing in the horizon and is statistically significant at the 1% level for all cases. Also, one can generally observe a monotonic pattern in the average excess returns of quintile portfolios, particularly for longer-term and total-horizon network risks. Consequently, currency portfolios based on the amount of transmitted shocks have the annualized Sharpe ratios ranging from 0.74 to 0.83 for the short- and long-term horizon connectedness. All strategies display a positive skew of their excess returns. Interestingly, this performance primarily stems from the exchange rate predictability, while the interest rate differential contributes less. For the from-directional case, the results indicate no clear patterns in the performance statistics of currency network strategies. Although the average excess returns of quintile and long-short portfolios tend to be positive, they remain insignificant at all conventional confidence levels. This ultimately leads to much smaller Sharpe ratios compared to those from other strategies.

Overall, the results presented in Table 2 suggest that the impact of a particular currency on exchange rates of other countries is the key to understanding the profitability of net-directional portfolios. Specifically, we document that the currencies transmitting more shocks to others tend to appreciate, leading to smaller currency risk premium. Unlike the carry trade strategy, we demonstrate that the stronger transmitters of causal shocks do not necessarily have the lowest interest rates. By connecting currency returns to network risk extracted from currency option data, we shed light on the novel risk that drives exchange rates above and beyond the existing risks capturing macroeconomic country-specific conditions and trade connections, among others.

**Table 3. Benchmark Strategies: Summary Statistics**

This table presents descriptive statistics (Panel A) and correlations (Panel B) between dollar (dol), carry trade (car), volatility (vol), volatility risk premium (vrp), momentum (mom) strategies and an equally weighted average of all currency benchmarks (1/N). Mean, standard deviation, and Sharpe ratio are annualized, but t-statistic of mean, skewness, kurtosis and the first-order autocorrelation are based on monthly returns. The t-statistics are based on [Newey and West \(1987\)](#) standard errors with [Andrews \(1991\)](#) optimal lag selection. The sample is from January 1996 to December 2013.

<b>Panel A: Benchmark strategies</b>						
	dol	car	vol	vrp	mom	1/N
mean (%)	1.60	7.29	2.28	1.66	3.64	3.30
t-stat	0.75	2.58	1.04	0.84	1.66	2.55
Sharpe	0.20	0.69	0.25	0.21	0.38	0.71
std (%)	8.16	10.52	8.98	8.04	9.49	4.62
skew	-0.60	-0.68	0.12	0.04	-0.17	-0.69
kurt	5.19	4.48	3.36	3.46	3.02	6.24
ac1	0.07	0.12	0.06	0.11	-0.04	0.14
<b>Panel B: Correlations</b>						
	dol	car	vol	vrp	mom	1/N
dol	1.00	0.33	0.61	-0.07	0.01	0.72
car	0.33	1.00	0.28	-0.29	0.23	0.68
vol	0.61	0.28	1.00	-0.17	-0.20	0.58
vrp	-0.07	-0.29	-0.17	1.00	-0.05	0.10
mom	0.01	0.23	-0.20	-0.05	1.00	0.42
1/N	0.72	0.68	0.58	0.10	0.42	1.00

### 4.3 Benchmark Strategies and Diversification Gains

We now study the relationship between network portfolios and existing benchmarks. We begin by reporting in [Table 3](#) summary statistics of the standard dollar, carry trade, volatility, variance risk premium, and momentum strategies, as well as an equally weighted average of all currency benchmarks. The carry trade and momentum strategies exhibit the highest Sharpe ratios of 0.69 and 0.38, with the former having a statistically significant mean excess return. However, both have a negative skewness, indicating the possibility of large losses. The last column shows limited diversification gains from equally combining all strategies as indicated by a tiny increase in the Sharpe ratio and a negative skewness of the “1/N” portfolio.

Next we examine how well the benchmark strategies can explain the network portfolios. We perform a two-step analysis. First, we compute the sample correlations between the excess returns of different strategies. Second, for network portfolios, we run contemporaneous regressions using their monthly returns as dependent variables and benchmark

strategies as independent variables. Tables 4 and 5 report the results of the two-stage procedure for investment strategies constructed in Sections 4.1 and 4.2.

Several observations in Table 4 are worth discussing. First, the currency portfolio returns sorted on aggregate connections tend to be more correlated with benchmark strategies than those based on causal linkages. Also, the negative correlations of aggregate (causal) network portfolios with vol and vrp (car and vol) provide the scope for diversification benefits. Second, the strength of the correlations directly translates into the significant coefficients for car, vol, and vrp (Panel B for total linkages). We can conclude that the significant portion of the excess returns obtained from aggregate network measures reflects interest rate differentials and global components of realized and implied currency variances. Third, once the contemporaneous effects are removed, none of the four factors appear to be significant (the right part of Panel B). Also, the predictive power of the four benchmarks for network portfolios drops dramatically as measured by the adjusted  $R^2$ , which range from 9.36% to 31.05% for aggregate linkages and are around 2% for causal linkages. Fourth, the resulting alphas for  $\mathcal{N}(S)$  are economically and statistically significant for both network risk measures. For instance, the annualized alphas of 5.00% and 6.58% are close to the average returns of 5.53% and 6.43% for the corresponding  $\mathcal{N}(S)$  strategies, that is, less than 10% of the network returns are explained by the four benchmark strategies. Panel C in Table 4 shows that the inclusion of the dollar slightly reduces the estimated alphas and increases the adjusted  $R^2$  statistics, but the significance of constants remains unchanged.

Table 5 replicates the analysis separately for the currency returns sorted on to-directional and from-directional causal connections. It demonstrates that the transmitted shocks in the global network of currency variances play the key role. Indeed, all  $\mathcal{T}(\mathcal{H}) : \mathcal{H} \in \{S, M, L, T\}$  generate highly significant performance, both economically and statistically, which cannot be understood through the lens of the benchmarks.

We further investigate the diversification benefits of network portfolios. For ease of presentation, we focus on short-term net-directional cases (both aggregate and causal networks). We implement a naive strategy combining the network portfolio and one of the benchmarks at a time with 0.5-0.5 weights. Table 6 shows that, for strategies based on

**Table 4. Net-directional Network Portfolios and Benchmark Strategies**

This table presents correlations (Panel A) and a contemporaneous regression (Panels B and C) of monthly returns of net-directional network portfolios ( $\mathcal{N}(\mathcal{H}) : \mathcal{H} \in \{S, M, L, T\}$ ) on benchmark strategies - dollar (dol), carry trade (car), volatility (vol), volatility risk premium (vrp), and momentum (mom). Constants reported in the "alpha (% annual)" row are expressed in percentage per annum. The numbers in rows with a grey font are t-statistics of estimates. The t-statistics are based on [Newey and West \(1987\)](#) standard errors with [Andrews \(1991\)](#) optimal lag selection. The last two rows report adjusted  $R^2$  values (in percentage) and the number of observations. The sample is from January 1996 to December 2013.

<b>Panel A: Correlations with trading strategies</b>								
	Aggregate linkages				Causal linkages			
	$\mathcal{N}(S)$	$\mathcal{N}(M)$	$\mathcal{N}(L)$	$\mathcal{N}(T)$	$\mathcal{N}(S)$	$\mathcal{N}(M)$	$\mathcal{N}(L)$	$\mathcal{N}(T)$
dol	-0.41	-0.25	-0.32	-0.41	-0.24	0.02	0.11	-0.05
car	0.20	0.46	0.36	0.29	-0.09	0.01	0.00	0.04
vol	-0.14	-0.13	-0.11	-0.20	-0.15	-0.12	-0.09	-0.12
vrp	-0.19	-0.29	-0.22	-0.26	0.09	0.04	0.08	-0.01
mom	0.14	0.21	0.12	0.18	0.11	0.17	0.18	0.20
<b>Panel B: Returns of network portfolios on benchmark strategies (without dollar)</b>								
	Aggregate linkages				Causal linkages			
	$\mathcal{N}(S)$	$\mathcal{N}(M)$	$\mathcal{N}(L)$	$\mathcal{N}(T)$	$\mathcal{N}(S)$	$\mathcal{N}(M)$	$\mathcal{N}(L)$	$\mathcal{N}(T)$
alpha (% annual)	5.00	2.28	1.37	3.53	6.58	3.06	2.28	4.46
	2.29	1.18	0.55	1.66	3.35	1.63	1.32	2.39
car	0.16	0.38	0.32	0.24	-0.05	0.00	-0.01	0.01
	1.71	6.22	2.81	2.60	-0.60	0.04	-0.16	0.24
vol	-0.21	-0.27	-0.25	-0.29	-0.09	-0.06	-0.03	-0.07
	-2.07	-3.83	-3.97	-4.00	-1.51	-1.19	-0.51	-1.35
vrp	-0.18	-0.21	-0.17	-0.23	0.06	0.03	0.07	-0.01
	-2.22	-2.42	-1.95	-2.67	0.69	0.45	1.05	-0.08
mom	0.04	0.02	-0.03	0.03	0.10	0.12	0.13	0.14
	0.48	0.36	-0.33	0.47	1.25	1.67	1.90	1.97
$R^2(\%)$	9.36	31.05	18.40	19.70	2.17	1.95	2.22	2.90
Number of obs.	215	215	215	215	215	215	215	215
<b>Panel C: Returns of network portfolios on benchmark strategies (with dollar)</b>								
	Aggregate linkages				Causal linkages			
	$\mathcal{N}(S)$	$\mathcal{N}(M)$	$\mathcal{N}(L)$	$\mathcal{N}(T)$	$\mathcal{N}(S)$	$\mathcal{N}(M)$	$\mathcal{N}(L)$	$\mathcal{N}(T)$
alpha (% annual)	4.36	1.83	0.80	2.92	6.31	3.17	2.48	4.44
	2.14	0.92	0.36	1.54	3.48	1.66	1.39	2.40
dol	-0.62	-0.44	-0.55	-0.59	-0.26	0.11	0.20	-0.01
	-7.43	-5.25	-5.64	-6.92	-2.70	1.37	2.52	-0.16
car	0.24	0.44	0.39	0.32	-0.02	-0.01	-0.04	0.02
	3.47	7.34	4.50	5.00	-0.26	-0.19	-0.59	0.26
vol	0.12	-0.03	0.05	0.02	0.05	-0.12	-0.14	-0.07
	1.21	-0.40	0.64	0.32	0.61	-1.94	-2.05	-1.06
vrp	-0.13	-0.17	-0.12	-0.18	0.08	0.02	0.05	0.00
	-1.78	-2.24	-1.55	-2.40	0.99	0.29	0.75	-0.06
mom	0.09	0.06	0.02	0.08	0.12	0.11	0.12	0.14
	1.46	1.14	0.21	1.53	1.46	1.60	1.81	1.98
$R^2(\%)$	30.21	41.84	34.11	38.97	5.89	2.38	4.97	2.45
Number of obs.	215	215	215	215	215	215	215	215

**Table 5. To- and From-directional Network Portfolios and Benchmark Strategies**

This table presents correlations (Panel A) and a contemporaneous regression (Panels B and C) of monthly returns of to- and from-directional network portfolios ( $\mathcal{T}(\mathcal{H})$  and  $\mathcal{F}(\mathcal{H}) : \mathcal{H} \in \{S, M, L, T\}$ ) on benchmark strategies - dollar (dol), carry trade (car), volatility (vol), volatility risk premium (vrp), and momentum (mom). Constants reported in the “alpha (% , annual)” row are expressed in percentage per annum. The numbers in rows with a grey font are t-statistics of estimates. The t-statistics are based on [Newey and West \(1987\)](#) standard errors with [Andrews \(1991\)](#) optimal lag selection. The last two rows report adjusted  $R^2$  values (in percentage) and the number of observations. The sample is from January 1996 to December 2013.

<b>Panel A: Correlations with trading strategies</b>								
	Causal linkages							
	$\mathcal{T}(S)$	$\mathcal{T}(M)$	$\mathcal{T}(L)$	$\mathcal{T}(T)$	$\mathcal{F}(S)$	$\mathcal{F}(M)$	$\mathcal{F}(L)$	$\mathcal{F}(T)$
dol	-0.27	-0.27	-0.20	-0.26	-0.35	-0.42	-0.27	-0.38
car	-0.09	-0.04	-0.03	-0.07	-0.08	-0.03	0.13	-0.05
vol	-0.14	-0.17	-0.19	-0.15	-0.14	-0.08	-0.12	-0.07
vrp	0.10	0.08	0.06	0.07	-0.03	-0.07	-0.09	-0.07
mom	0.14	0.16	0.14	0.14	-0.14	-0.09	-0.01	-0.11
<b>Panel B: Returns of network portfolios on benchmark strategies (without dollar)</b>								
	Causal linkages							
	$\mathcal{T}(S)$	$\mathcal{T}(M)$	$\mathcal{T}(L)$	$\mathcal{T}(T)$	$\mathcal{F}(S)$	$\mathcal{F}(M)$	$\mathcal{F}(L)$	$\mathcal{F}(T)$
alpha (% , annual)	6.14	6.39	6.53	6.05	1.67	2.13	0.44	3.34
	3.20	3.15	3.52	3.07	1.03	1.20	0.27	1.99
car	-0.06	-0.02	0.00	-0.04	-0.01	0.00	0.13	-0.01
	-0.72	-0.24	-0.01	-0.51	-0.13	0.04	2.31	-0.19
vol	-0.07	-0.11	-0.14	-0.09	-0.15	-0.10	-0.17	-0.09
	-1.17	-1.67	-2.24	-1.42	-2.16	-1.12	-1.89	-1.08
vrp	0.07	0.06	0.04	0.04	-0.07	-0.09	-0.07	-0.09
	0.73	0.60	0.46	0.47	-1.05	-1.44	-1.11	-1.43
mom	0.13	0.12	0.09	0.11	-0.14	-0.10	-0.08	-0.10
	1.68	1.59	1.17	1.40	-2.72	-1.65	-1.29	-1.94
$R^2(\%)$	2.81	2.93	3.12	2.23	3.57	0.85	3.97	1.08
Number of obs.	215	215	215	215	215	215	215	215
<b>Panel C: Returns of network portfolios on benchmark strategies (with dollar)</b>								
	Causal linkages							
	$\mathcal{T}(S)$	$\mathcal{T}(M)$	$\mathcal{T}(L)$	$\mathcal{T}(T)$	$\mathcal{F}(S)$	$\mathcal{F}(M)$	$\mathcal{F}(L)$	$\mathcal{F}(T)$
alpha (% , annual)	5.81	6.07	6.36	5.74	1.29	1.54	0.12	2.84
	3.20	3.20	3.53	3.09	0.77	0.96	0.07	1.81
dol	-0.33	-0.31	-0.16	-0.30	-0.37	-0.57	-0.31	-0.49
	-3.04	-3.38	-1.63	-3.51	-5.75	-6.63	-3.59	-5.08
car	-0.02	0.02	0.02	-0.01	0.04	0.08	0.17	0.05
	-0.27	0.29	0.26	-0.07	0.78	1.56	3.14	1.06
vol	0.10	0.06	-0.05	0.07	0.05	0.20	0.00	0.17
	1.10	0.66	-0.61	0.85	0.67	2.20	-0.01	1.87
vrp	0.10	0.08	0.06	0.07	-0.03	-0.04	-0.04	-0.05
	1.11	0.96	0.61	0.80	-0.58	-0.78	-0.74	-0.92
mom	0.16	0.14	0.11	0.14	-0.11	-0.05	-0.05	-0.06
	1.96	1.84	1.30	1.66	-2.27	-1.05	-0.93	-1.30
$R^2(\%)$	8.61	8.28	4.32	7.24	13.38	22.73	10.86	18.09
Number of obs.	215	215	215	215	215	215	215	215

**Table 6. Benchmark Strategies: Diversification Gains**

This table presents the impact of adding short-term net-directional strategy ( $\mathcal{N}(S)$ ) to benchmark strategies - dollar (dol), carry trade (car), volatility (vol), volatility risk premium (vrp), and momentum (mom). We construct a naive 50%-50% portfolio of  $\mathcal{N}(S)$  and one of benchmark strategies. The “1/N” column presents the statistics of an equally weighted portfolio of all benchmarks and a network strategy. Panel A (B) reports the results for the case of aggregate (causal) linkages. Mean, standard deviation, and Sharpe ratio are annualized, but t-statistic of mean, skewness, kurtosis and the first-order autocorrelation are based on monthly returns. The t-statistics are based on [Newey and West \(1987\)](#) standard errors with [Andrews \(1991\)](#) optimal lag selection. The last row in each panel shows the percentage increase in the Sharpe ratio of a diversified portfolio relative to the original benchmark strategy. The sample is from January 1996 to December 2013.

<b>Panel A: Including short-term net-directional strategy: aggregate linkages</b>						
	dol	car	vol	vrp	mom	1/N
	+ $\mathcal{N}(S)$					
mean (%)	3.56	6.41	3.91	3.59	4.58	4.41
t-stat	2.75	3.13	2.79	3.00	2.59	3.49
Sharpe	0.78	0.87	0.68	0.68	0.67	0.96
std (%)	4.55	7.39	5.72	5.26	6.80	4.60
skew	-0.17	-0.21	0.07	-0.22	-0.26	-0.20
kurt	3.67	3.41	5.83	4.00	3.27	4.17
ac1	0.13	0.15	0.00	0.00	0.02	0.09
% $\Delta$ Sharpe	290.00	26.09	172.00	223.81	76.32	35.21
<b>Panel B: Including short-term net-directional strategy: causal linkages</b>						
	dol	car	vol	vrp	mom	1/N
	+ $\mathcal{N}(S)$					
mean (%)	4.01	6.86	4.36	4.05	5.04	4.86
t-stat	3.24	4.13	3.07	3.21	3.76	4.73
Sharpe	0.80	1.08	0.78	0.68	0.77	1.10
std (%)	5.00	6.34	5.56	5.96	6.57	4.43
skew	-0.60	-0.28	0.11	0.34	0.14	-0.15
kurt	3.53	3.87	3.28	4.79	4.47	3.56
ac1	0.00	0.13	0.04	-0.03	-0.14	-0.03
% $\Delta$ Sharpe	300.00	56.52	212.00	223.81	102.63	54.93

aggregate connections, the resulting Sharpe ratios become considerably higher relative to the individual benchmarks, with the increase ranging from 26% for car and to well above 200% for dol and vrp. As can be expected from the correlation analysis, the causal network portfolio leads to better diversification benefits. For instance, the allocation in  $\mathcal{N}(S)$  and car generates a ratio of 1.08, which is 56.52% higher than the original carry trade.

Finally, we now perform the allocation analysis of selected portfolios:  $\mathcal{N}(S)$  for causal linkages, car, vol, vrp, and mom. Table 7 reports the fraction of months each investment strategy goes long (the “Buy” columns) or short (the “Sell” columns) in each currency. We

**Table 7. Allocation Analysis for the Network Portfolio and Benchmark Strategies**

This table presents an allocation analysis of a short-term net-directional network portfolio based on causal linkages ( $\mathcal{N}(S)$ ) and carry trade (car), volatility (vol), volatility risk premium (vrp), and momentum (mom) strategies. The “Buy” and “Sell” columns report the fraction of months each currency belongs to the long and short positions of portfolios considered. The “Diff” column for each benchmark strategy reports the fraction of months the position for a particular currency is different from the one in  $\mathcal{N}(S)$ . The bottom row reports the average fraction across the currencies. The sample is from January 1996 to December 2013.

	$\mathcal{N}(S)$		car			vol			vrp			mom		
	Buy	Sell	Buy	Sell	Diff	Buy	Sell	Diff	Buy	Sell	Diff	Buy	Sell	Diff
Australia	0.25	0.15	0.00	0.00	0.40	0.26	0.02	0.53	0.28	0.10	0.53	0.25	0.16	0.57
Brazil	0.41	0.06	0.67	0.00	0.26	0.23	0.07	0.47	0.12	0.36	0.53	0.35	0.10	0.38
Canada	0.10	0.25	0.00	0.07	0.37	0.02	0.54	0.60	0.24	0.08	0.47	0.17	0.20	0.52
Czech Republic	0.06	0.12	0.00	0.07	0.23	0.17	0.01	0.28	0.17	0.08	0.29	0.09	0.09	0.23
Denmark	0.00	0.15	0.00	0.10	0.20	0.05	0.07	0.25	0.07	0.08	0.28	0.09	0.16	0.33
Euro Area	0.01	0.17	0.00	0.26	0.24	0.05	0.06	0.27	0.09	0.08	0.30	0.06	0.15	0.25
Hungary	0.13	0.16	0.53	0.00	0.48	0.34	0.00	0.48	0.16	0.20	0.42	0.24	0.10	0.38
Japan	0.27	0.22	0.00	1.00	0.78	0.24	0.13	0.50	0.26	0.23	0.58	0.16	0.40	0.65
Mexico	0.59	0.12	0.36	0.00	0.59	0.09	0.36	0.71	0.11	0.40	0.67	0.27	0.25	0.56
New Zealand	0.13	0.20	0.24	0.00	0.38	0.40	0.02	0.55	0.34	0.18	0.54	0.27	0.14	0.51
Norway	0.04	0.20	0.08	0.00	0.29	0.19	0.04	0.40	0.23	0.13	0.51	0.13	0.12	0.40
Poland	0.27	0.09	0.18	0.00	0.34	0.40	0.03	0.52	0.21	0.24	0.55	0.26	0.11	0.40
Singapore	0.07	0.27	0.00	0.48	0.36	0.00	0.66	0.40	0.10	0.04	0.34	0.04	0.15	0.38
South Africa	0.33	0.25	0.92	0.00	0.64	0.59	0.14	0.80	0.21	0.52	0.67	0.31	0.27	0.60
South Korea	0.40	0.00	0.00	0.00	0.40	0.02	0.27	0.45	0.07	0.20	0.44	0.11	0.08	0.38
Sweden	0.06	0.16	0.00	0.12	0.28	0.19	0.02	0.34	0.23	0.12	0.47	0.10	0.16	0.40
Switzerland	0.06	0.30	0.00	0.98	0.69	0.19	0.03	0.49	0.27	0.10	0.59	0.14	0.25	0.53
Taiwan	0.09	0.35	0.00	0.41	0.33	0.00	0.71	0.37	0.10	0.09	0.43	0.05	0.27	0.43
Turkey	0.17	0.20	0.55	0.00	0.38	0.12	0.10	0.39	0.08	0.23	0.34	0.19	0.11	0.39
United Kingdom	0.11	0.14	0.01	0.06	0.32	0.01	0.27	0.33	0.21	0.09	0.39	0.18	0.16	0.48
Average					0.40			0.46			0.47			0.44

also compute the fraction of months when the currency position in  $\mathcal{N}(S)$  is different from the currency allocation in the benchmarks (the “Diff” columns). The bottom row shows the average fraction of “Diff” statistics across the currencies.

Table 7 demonstrates significant differences across strategies and countries. For instance, the network strategy on average buys or sells alternative currencies in 40%, 46%, 47%, and 44% of the time relative to the carry trade, volatility, variance risk premium, and momentum strategies. The countries whose allocations differ most in their distributions relative to  $\mathcal{N}(S)$  are Japan and Switzerland for the carry trade, South Africa and Mexico for volatility, Mexico and South Africa for variance risk premium, Japan and South Africa for momentum. Most notably, if we sort the currencies according to interest rate differentials, we would have bought South African rand (ZAR) in 92% of months and would have always kept Japanese yen (JPY) in the short position. In contrast, our causal net-directional strategy buys and sells JPY in 27% and 22% of the time and ZAR in 33% and 25%.



#### 4.4 Daily and Weekly Frequencies

Given the availability of the network estimates at the daily frequency, it is reasonable to ask whether the profits of network strategies are sensitive to the frequency of rebalancing. We therefore construct horizon specific net-directional network portfolios (aggregate and causal linkages) and the benchmark strategies at the daily and weekly frequencies. Specifically, we use the daily network estimates from the core analysis and sample the daily or end-of-week observations to construct long-short portfolios. The realized volatility and variance risk premium are computed on the rolling one-month window, while the currency momentum is computed over the rolling six-month horizon. For daily and weekly frequencies, Tables 8 and 9 report summary statistics of network portfolios (Panels A and B), regression outputs with the network excess returns as a dependent variable and benchmarks as independent variables (Panel C).

Several interesting observations emerge from this investigation. First, the Sharpe ratios of short-term (long-term) network portfolios sorted on aggregate connectedness decline (increase) with more frequent rebalancing, whereas the medium-term and total connections are priced similarly. Second, the Sharpe ratios of the causal network strategies for all horizons increase substantially for weekly and especially daily frequency: 0.99, 0.57, 0.57, 0.64 (weekly) and 1.13, 0.72, 0.71, 0.84 (daily) for  $\mathcal{N}(\mathcal{H}) : \mathcal{H} \in \{S, M, L, T\}$ , respectively. Thus, we similarly document the downward-sloping term structure of causal net-directional network linkages, but we find that trading medium- and long-term connectedness now becomes more profitable. Third, among the benchmarks, the carry trade is the only strategy consistently generating high Sharpe ratios (0.65 and 0.70 for the daily and weekly frequencies).

Finally, the contemporaneous regressions indicate that the estimated alphas exhibit similar patterns to the risk-adjusted performance measured by the Sharpe ratios. Specifically, the abnormal returns of aggregate network strategies relative to the benchmarks seem to increase more significantly for longer network horizons than for shorter ones, 2.18% and 3.95% per annum for  $\mathcal{N}(L)$  and 3.20% and 3.68% per annum for  $\mathcal{N}(S)$  with weekly and daily frequencies, respectively. The alphas of strategies employing causal linkages strongly increase in magnitude and become highly significant, both economically and statistically: 5.71% per annum (a t-stat of 3.07) for  $\mathcal{N}(L)$  and 10.36% per annum (a t-stat of 5.35) for

**Table 8. Daily Frequency**

This table presents a robustness analysis of currency strategies implemented on a daily frequency. It reports descriptive statistics of net-directional network portfolios (Panel A) and benchmark strategies (Panel B), and a contemporaneous regression (Panel C) of daily returns of net-directional network portfolios ( $\mathcal{N}(\mathcal{H}) : \mathcal{H} \in \{S, M, L, T\}$ ) on benchmark strategies - dollar (dol), carry trade (car), volatility (vol), volatility risk premium (vrp), and momentum (mom). In Panels A and B, mean, standard deviation, and Sharpe ratio are annualized, but t-statistic of mean, skewness, kurtosis and the first-order autocorrelation are based on daily returns. In Panel C, constants reported in the “alpha (% , annual)” row are expressed in percentage per annum. The numbers in rows with a grey font are t-statistics of estimates. The t-statistics are based on [Newey and West \(1987\)](#) standard errors with [Andrews \(1991\)](#) optimal lag selection. The last two rows report adjusted  $R^2$  values (in percentage) and the number of observations. The sample is from January 1996 to December 2013.

<b>Panel A: Performance of network portfolios</b>								
	Aggregate linkages				Causal linkages			
	$\mathcal{N}(S)$	$\mathcal{N}(M)$	$\mathcal{N}(L)$	$\mathcal{N}(T)$	$\mathcal{N}(S)$	$\mathcal{N}(M)$	$\mathcal{N}(L)$	$\mathcal{N}(T)$
mean (%)	4.22	4.72	4.46	4.57	9.91	6.13	5.73	7.02
t-stat	2.04	2.34	2.10	2.14	4.96	3.14	3.02	3.65
Sharpe	0.47	0.50	0.47	0.47	1.13	0.72	0.71	0.84
std (%)	9.02	9.41	9.50	9.65	8.81	8.51	8.07	8.41
skew	-0.18	-0.08	0.17	0.38	0.36	0.39	0.36	0.06
kurt	5.52	7.19	11.59	11.96	17.92	15.28	8.70	14.76
ac1	-0.05	-0.05	-0.07	-0.09	-0.04	-0.03	0.01	-0.03

<b>Panel B: Performance of benchmark strategies</b>						
	dol	car	vol	vrp	mom	
mean (%)	1.62	7.23	1.86	6.13	0.40	
t-stat	0.85	2.87	0.84	2.86	0.17	
Sharpe	0.21	0.65	0.18	0.65	0.04	
std (%)	7.64	11.14	10.47	9.38	10.49	
skew	-0.03	-0.67	-0.05	0.61	-0.48	
kurt	8.08	11.21	8.40	9.57	9.89	
ac1	0.04	-0.01	-0.04	-0.03	0.02	

<b>Panel C: Returns of network portfolios on benchmark strategies</b>								
	Aggregate linkages				Causal linkages			
	$\mathcal{N}(S)$	$\mathcal{N}(M)$	$\mathcal{N}(L)$	$\mathcal{N}(T)$	$\mathcal{N}(S)$	$\mathcal{N}(M)$	$\mathcal{N}(L)$	$\mathcal{N}(T)$
alpha (% , annual)	3.68	4.62	3.95	4.64	10.36	6.83	5.71	7.38
	2.04	2.64	2.09	2.50	5.35	3.46	3.07	4.00
dol	-0.55	-0.65	-0.58	-0.62	-0.09	0.06	0.12	0.02
	-13.93	-16.13	-13.63	-15.64	-2.50	1.41	2.89	0.41
car	0.29	0.26	0.26	0.22	0.00	-0.08	-0.03	-0.03
	11.19	6.36	6.05	4.94	0.11	-1.83	-1.01	-0.69
vol	-0.07	-0.01	-0.06	-0.09	-0.26	-0.19	-0.18	-0.23
	-1.76	-0.31	-1.36	-1.95	-7.06	-4.68	-5.48	-6.12
vrp	-0.09	-0.12	-0.06	-0.08	0.02	0.01	0.05	0.03
	-3.21	-3.83	-1.62	-2.31	0.62	0.48	2.13	0.97
mom	0.00	0.09	0.11	0.11	0.15	0.17	0.13	0.16
	0.02	3.16	2.85	2.67	4.69	5.51	4.84	5.26
$R^2(\%)$	29.31	31.73	28.58	31.92	19.97	14.47	8.80	15.83
Number of obs.	4457	4457	4457	4457	4457	4457	4457	4457

**Table 9. Weekly Frequency**

This table presents a robustness analysis of currency strategies implemented on a weekly frequency. The table reports descriptive statistics of net-directional network portfolios (Panel A) and benchmark strategies (Panel B), and a contemporaneous regression (Panel C) of weekly returns of net-directional network portfolios ( $\mathcal{N}(\mathcal{H}) : \mathcal{H} \in \{S, M, L, T\}$ ) on benchmark strategies - dollar (dol), carry trade (car), volatility (vol), volatility risk premium (vrp), and momentum (mom). In Panels A and B, mean, standard deviation, and Sharpe ratio are annualized, but t-statistic of mean, skewness, kurtosis and the first-order autocorrelation are based on weekly returns. In Panel C, constants reported in the “alpha (% annual)” row are expressed in percentage per annum. The numbers in rows with a grey font are t-statistics of estimates. The t-statistics are based on [Newey and West \(1987\)](#) standard errors with [Andrews \(1991\)](#) optimal lag selection. The last two rows report adjusted  $R^2$  values (in percentage) and the number of observations. The sample is from January 1996 to December 2013.

<b>Panel A: Performance of network portfolios</b>								
	Aggregate linkages				Causal linkages			
	$\mathcal{N}(S)$	$\mathcal{N}(M)$	$\mathcal{N}(L)$	$\mathcal{N}(T)$	$\mathcal{N}(S)$	$\mathcal{N}(M)$	$\mathcal{N}(L)$	$\mathcal{N}(T)$
mean (%)	4.09	3.60	3.22	4.13	8.70	4.78	4.61	5.35
t-stat	1.90	1.83	1.59	2.03	4.29	2.66	2.79	2.99
Sharpe	0.49	0.42	0.36	0.47	0.99	0.57	0.57	0.64
std (%)	8.41	8.57	8.89	8.78	8.76	8.43	8.09	8.35
skew	-0.12	-0.19	0.56	0.56	1.41	0.89	0.46	0.40
kurt	3.76	4.41	9.75	8.44	20.74	13.54	8.45	9.65
ac1	0.04	-0.06	-0.05	-0.06	-0.05	-0.09	-0.07	-0.11

<b>Panel B: Performance of benchmark strategies</b>						
	dol	car	vol	vrp	mom	
mean (%)	1.61	7.38	0.31	2.58	2.51	
t-stat	0.83	2.96	0.17	1.02	1.13	
Sharpe	0.20	0.70	0.04	0.24	0.24	
std (%)	7.87	10.59	7.80	10.66	10.47	
skew	-0.51	-0.82	0.49	0.44	-0.72	
kurt	6.75	7.87	7.91	6.59	8.63	
ac1	-0.02	-0.09	-0.03	-0.08	-0.15	

<b>Panel C: Returns of network portfolios on benchmark strategies</b>								
	Aggregate linkages				Causal linkages			
	$\mathcal{N}(S)$	$\mathcal{N}(M)$	$\mathcal{N}(L)$	$\mathcal{N}(T)$	$\mathcal{N}(S)$	$\mathcal{N}(M)$	$\mathcal{N}(L)$	$\mathcal{N}(T)$
alpha (% annual)	3.20	2.59	2.18	3.37	7.77	4.23	3.05	4.45
	1.62	1.48	1.15	1.95	3.70	2.09	1.81	2.50
dol	-0.64	-0.62	-0.51	-0.66	-0.13	0.05	0.18	-0.01
	-10.68	-10.54	-9.25	-10.34	-1.74	0.64	2.46	-0.10
car	0.28	0.27	0.23	0.23	0.02	-0.07	0.03	-0.02
	5.98	5.48	3.92	4.36	0.34	-0.89	0.63	-0.30
vol	0.08	-0.01	-0.08	0.03	0.06	0.06	0.06	0.07
	1.10	-0.13	-0.99	0.35	0.95	1.23	1.05	1.33
vrp	-0.09	-0.07	-0.01	-0.05	0.23	0.20	0.27	0.21
	-1.11	-0.97	-0.07	-0.61	3.54	3.02	3.98	3.15
mom	0.02	0.08	0.08	0.10	0.15	0.18	0.13	0.19
	0.48	2.11	1.96	2.14	3.29	4.31	2.31	4.63
$R^2(\%)$	26.63	28.63	21.69	29.70	18.21	16.36	11.68	18.36
Number of obs.	890	890	890	890	890	890	890	890

$\mathcal{N}(S)$  with the daily rebalancing.

In sum, the profits of network strategies strongly increase when we move to daily portfolio constructions. The improvement is especially pronounced for causal connections. Hence, unlike most of the standard benchmark strategies, investing in currencies based on the network risk information is profitable regardless of the trader’s rebalancing horizons.

#### 4.5 Transaction Costs and Subsamples

We perform two additional robustness checks. First, we report the performance statistics for the network excess returns net of transaction costs. Since the bid-ask quotes for exchange rates are available from Barclays and Reuters, we incorporate those into the currency excess returns following [Menkhoff et al. \(2012b\)](#).<sup>13</sup> It is worth noting that the bid-ask data are for quoted spreads and not effective spreads. [Lyons et al. \(2001\)](#) suggest that the bid-ask spread data are based on the indicative spreads and, therefore, might be too high relative to actual effective ones. Following the existing literature (see, for example, [Goyal and Saretto \(2009\)](#), [Menkhoff et al. \(2012a, 2017\)](#), and [Colacito et al. \(2020\)](#) among others), we employ 50% of quoted bid-ask spreads in our calculations.<sup>14</sup>

Table 10 reports summary statistics of the excess returns of currency network portfolios adjusted for transaction costs. In comparison with the results shown in Tables 1 and 2, the Sharpe ratios of the  $\mathcal{N}(S)$  portfolios based on total and causal connectedness decline from 0.65 and 0.80 to 0.54 and 0.66, respectively. The to-directional network portfolios experience a comparable drop in their performances, with the Sharpe ratios ranging from 0.61 to 0.70. Hence, although the returns are somewhat lower after accounting for transaction costs, the network portfolios still exhibit both economically and statistically significant performance.

Second, we divide the whole sample into half and look at the performance of the network strategies for the subperiods 1996-2004 and 2005-2013. The availability and the amount of currency options vary over time and countries, with sparser data for the first half of the sample. As might be expected, with less precise estimates of the forward-looking currency variances, trading network risks is less profitable from 1996 to 2004, though the short-term net-directional and especially to-directional portfolios still exhibit high Sharpe

---

<sup>13</sup>Please see Appendix C for more details on how we account for transaction costs.

<sup>14</sup>[Gilmore and Hayashi \(2011\)](#) suggest that the effective bid-ask spreads could be even lower than 50%, while [Cespa et al. \(2019\)](#) suggest a 25% rule for the data from 2011.

**Table 10. Transaction Costs**

This table presents descriptive statistics for long-short net-directional (Panel A), to-directional and from-directional (Panel B) network portfolios adjusted for transaction costs. Mean, standard deviation, and Sharpe ratio are annualized, but t-statistic of mean, skewness, kurtosis and the first-order autocorrelation are based on monthly returns. The t-statistics are based on [Newey and West \(1987\)](#) standard errors with [Andrews \(1991\)](#) optimal lag selection. The sample is from January 1996 to December 2013.

<b>Panel A: Net-directional network portfolios</b>								
	Aggregate linkages				Causal linkages			
	$\mathcal{N}(S)$	$\mathcal{N}(M)$	$\mathcal{N}(L)$	$\mathcal{N}(T)$	$\mathcal{N}(S)$	$\mathcal{N}(M)$	$\mathcal{N}(L)$	$\mathcal{N}(T)$
mean (%)	4.60	3.26	1.86	3.45	5.37	2.37	1.70	3.88
t-stat	2.06	1.44	0.81	1.52	3.19	1.46	1.14	2.40
Sharpe	0.54	0.39	0.21	0.41	0.66	0.33	0.24	0.52
std (%)	8.49	8.29	8.71	8.43	8.07	7.21	7.07	7.43
skew	-0.41	-0.41	-0.01	-0.30	0.93	0.07	0.02	-0.33
kurt	4.25	4.54	5.12	4.09	6.83	3.41	3.45	4.89
ac1	0.10	0.20	0.09	0.12	-0.15	-0.04	-0.05	-0.04
<b>Panel B: To- and from-directional network portfolios</b>								
	Causal linkages				Causal linkages			
	$\mathcal{T}(S)$	$\mathcal{T}(M)$	$\mathcal{T}(L)$	$\mathcal{T}(T)$	$\mathcal{F}(S)$	$\mathcal{F}(M)$	$\mathcal{F}(L)$	$\mathcal{F}(T)$
mean (%)	5.03	5.46	5.56	4.93	-0.47	0.29	-0.52	1.41
t-stat	3.03	3.09	3.38	2.90	-0.30	0.18	-0.32	0.90
Sharpe	0.61	0.67	0.70	0.61	-0.06	0.04	-0.07	0.19
std (%)	8.28	8.13	7.98	8.04	7.26	7.57	7.22	7.39
skew	0.33	0.23	0.24	0.31	0.03	-0.03	0.01	-0.30
kurt	5.26	3.94	4.02	4.24	3.64	3.91	3.21	4.23
ac1	-0.15	-0.11	-0.19	-0.13	-0.11	-0.04	-0.07	-0.04

ratios. With more data available from 2005 to 2013, the network strategies generate Sharpe ratios ranging from 0.65 to 1.18. In particular, the risk-adjusted return of the causal  $\mathcal{N}(S)$  portfolio is 0.92 with a skewness of 1.78 in the second half.

## 5 Asset Pricing

This section presents the cross-sectional asset-pricing tests performed on the excess returns of network portfolios. Motivated by the previous results, we focus on two sets of test portfolios: the cross-section of currency returns sorted by the short-term net-directional network measures built from aggregate and causal linkages.

### 5.1 Methodology

Cross-sectional asset pricing tests are based on a stochastic discount factor (SDF) approach ([Cochrane, 2005](#)). In our application, we adopt the setting of [Lustig et al. \(2011\)](#) for the network portfolios of our paper. In the absence of arbitrage opportunities, the excess

**Table 11. Subsamples**

This table presents a robustness analysis of currency strategies for subsamples from January 1996 to December 2004 and from January 2005 to December 2013. The table reports descriptive statistics of net-directional network portfolios from aggregate (Panel A) and causal (Panel B) connectedness. Mean, standard deviation, and Sharpe ratio are annualized, but t-statistic of mean, skewness, kurtosis and the first-order autocorrelation are based on monthly returns. The t-statistics are based on [Newey and West \(1987\)](#) standard errors with [Andrews \(1991\)](#) optimal lag selection.

<b>Panel A: Aggregate linkages</b>								
	1996-2004				2005-2013			
	$\mathcal{N}(S)$	$\mathcal{N}(M)$	$\mathcal{N}(L)$	$\mathcal{N}(T)$	$\mathcal{N}(S)$	$\mathcal{N}(M)$	$\mathcal{N}(L)$	$\mathcal{N}(T)$
mean (%)	5.22	3.73	0.60	3.76	5.83	4.59	4.89	4.92
t-stat	1.51	0.98	0.16	1.01	2.04	1.86	1.99	1.91
Sharpe	0.57	0.39	0.06	0.40	0.73	0.65	0.65	0.67
std (%)	9.08	9.44	9.73	9.40	7.96	7.02	7.54	7.39
skew	-0.11	-0.49	-0.37	-0.52	-0.78	-0.11	0.97	0.25
kurt	2.82	4.42	3.84	3.78	6.52	3.54	7.01	4.12
ac1	0.12	0.25	0.19	0.20	0.07	0.10	-0.09	-0.03
<b>Panel B: Causal linkages</b>								
	1996-2004				2005-2013			
	$\mathcal{N}(S)$	$\mathcal{N}(M)$	$\mathcal{N}(L)$	$\mathcal{N}(T)$	$\mathcal{N}(S)$	$\mathcal{N}(M)$	$\mathcal{N}(L)$	$\mathcal{N}(T)$
mean (%)	6.07	0.30	0.61	2.39	6.79	6.51	4.83	7.37
t-stat	2.25	0.14	0.30	1.00	3.27	2.83	2.28	3.52
Sharpe	0.69	0.04	0.08	0.28	0.92	0.99	0.75	1.18
std (%)	8.74	7.74	7.64	8.45	7.42	6.57	6.43	6.25
skew	0.44	0.09	0.04	-0.45	1.78	0.20	0.08	0.31
kurt	3.61	3.25	2.89	4.76	12.48	3.62	4.34	3.32
ac1	-0.15	-0.14	-0.16	-0.08	-0.15	0.06	0.08	0.02
	1996-2004				2005-2013			
	$\mathcal{T}(S)$	$\mathcal{T}(M)$	$\mathcal{T}(L)$	$\mathcal{T}(T)$	$\mathcal{T}(S)$	$\mathcal{T}(M)$	$\mathcal{T}(L)$	$\mathcal{T}(T)$
mean (%)	6.64	6.38	7.10	6.40	5.57	6.65	6.13	5.59
t-stat	2.56	2.24	2.72	2.29	2.67	3.11	2.98	2.81
Sharpe	0.73	0.69	0.77	0.69	0.76	0.97	0.93	0.83
std (%)	9.15	9.28	9.22	9.23	7.34	6.85	6.58	6.71
skew	0.07	0.10	0.18	0.09	0.86	0.58	0.38	0.85
kurt	3.57	3.52	3.67	3.48	8.70	4.19	3.79	5.53
ac1	-0.15	-0.12	-0.21	-0.12	-0.15	-0.09	-0.14	-0.15

returns  $rx_{t+1}^j$  of a portfolio  $j$  have a zero price and satisfy the following Euler equation:

$$\mathbb{E}_t \left( M_{t+1} rx_{t+1}^j \right) = 0, \quad (11)$$

in which  $M_{t+1}$  is the SDF. Following a common approach in the literature, we consider the linear specification of  $M_{t+1}$  :

$$M_{t+1} = 1 - b'(f_{t+1} - \mu_f), \quad (12)$$

in which  $f_{t+1}$  is the vector of pricing factors,  $b$  is the vector of SDF loadings,  $\mu_f$  is the vector of factor means.<sup>15</sup> Combining Eq. (11)-(12), one can obtain a beta pricing model  $\mathbb{E}_t \left( rx_{t+1}^j \right) = \lambda' \beta^j$ , in which  $\lambda$  is the vector of the factor risk prices, and  $\beta^j$  is the vector of the risk quantities. The latter are also the regression coefficients of excess returns  $rx_{t+1}^j$  on the risk factors  $f_{t+1}$ . Further, the SDF loadings and factor risk prices are related to each other via the equation  $\lambda = \Sigma_f b$ , where  $\Sigma_f = \mathbb{E}_t \left[ (f_{t+1} - \mu_f)(f_{t+1} - \mu_f)'\right]$  is the variance-covariance matrix of risk factors.

We test a variety of linear factor models for the cross-section of network portfolios. For each model specification, we estimate the factor loadings via the one-step generalized method of moments (GMM) with the identity weighting matrix (Hansen, 1982). We simultaneously estimate the unknown factor means by adding the corresponding restrictions to a set of moments for the pricing errors. Since we are interested in testing whether a particular linear model explains the cross-section of expected currency excess returns, we implement a GMM estimation based on unconditional moments without instruments. Having estimated SDF loadings, we recover the risk prices from the identity  $\lambda = \Sigma_f b$  and calculate their standard errors using the Delta method. The t-statistics of  $b$ 's and  $\lambda$ 's are based on Newey and West (1987) standard errors with Andrews (1991) optimal lag selection. We evaluate the fit of linear pricing models by using three statistics: the cross-sectional  $R^2$ , root mean squared pricing error (RMSE), and the Hansen and Jagannathan (1997) distance ( $HJ_{\text{dist}}$ ). We further calculate the simulated p-values for testing the null hypothesis that the pricing errors equal zero, i.e.  $HJ_{\text{dist}}$  equals zero. Following Jagannathan and Wang (1996) and Kan and Robotti (2008), we obtain the simulated p-values by using a weighted sum of independent random variables from  $\chi^2(1)$  distribution.<sup>16</sup>

## 5.2 Principal Component Analysis on Network Portfolios

Before performing formal cross-sectional asset pricing tests, we investigate whether average network excess returns stemming from short-term net-directional connectedness can be associated with a small group of risk factors. Following Lustig et al. (2011), we conduct a principal component (PC) decomposition of currency network portfolios formed

---

<sup>15</sup>Other prominent examples considering a linear SDF specification include Menkhoff et al. (2012a), Della Corte et al. (2016), Colacito et al. (2020) and Della Corte et al. (2020) among many others.

<sup>16</sup>Appendix B provides a detailed description of the GMM estimation and test statistics.



on aggregate or causal linkages. Further, we study the correlations of principal components with the network and benchmark strategies.

Table 12 presents the results. There are several common and distinctive features of two cross-sections. First, the PC loadings indicate a strong factor structure in both groups of network cross-sections. The first principal component (PC1) accounts for most of the time-variation in quintile portfolios and has similar loadings across the five portfolios. The second principal component (PC2) in turn displays a pronounced monotonic pattern in loadings as we move from  $\mathcal{P}_1$  to  $\mathcal{P}_5$ : the increasing pattern for aggregate linkages and the decreasing tendency for causal connections. Second, the first two principal components explain around 84% and 86% of the common variation in network portfolios formed on aggregate or causal connections. Further, they exhibit similar correlations with risk factors. PC1 is perfectly correlated with the dollar factor in both cases. PC2 exhibits the strongest correlation with the network portfolio, though the relationship is of the opposite sign in the two cases. In relative terms, for causal linkages, the correlation of PC2 with  $\mathcal{N}(S)$  is strongly dominant, whereas PC2 from aggregate connectedness almost equally correlates with  $\mathcal{N}(S)$  and the carry trade factor. Finally, the starkest difference between the two portfolio groups is related to loadings of the third principal component (PC3), which show no visible pattern in Panel A but display monotonicity in Panel B. In the latter case, PC3 strongly relates to the network and carry trade risk factors.

Overall, the results in Table 12 suggest that the network-sorted portfolios can indeed be summarized by a small number of risk factors. We can approximate the first using the average returns across spot currency portfolios and interpret it as a “level” factor. We can approximate the second using the spread between  $\mathcal{P}_5$  and  $\mathcal{P}_1$  portfolios and interpret it as a “level” factor. For the cross-section of causal network portfolios, the results are suggestive of an additional “level” factor, which is strongly correlated with the carry trade.

### 5.3 Cross-Sectional Regressions

We now turn to the formal investigation of network portfolios following the methodology outlined in Section 5.1. Motivated by the principal component analysis in Section 5.2, we consider (A1) a variety of two-factor linear models for the cross-section of excess returns sorted on aggregate connectedness and (A2) a variety of two- and three-factor lin-



**Table 12. Principal Components: Short-term Net-directional Network Portfolios**

This table presents the loadings of principal components ( $PC_i : i = 1, \dots, 5$ ) for quintile portfolios ( $\mathcal{P}_i : i = 1, \dots, 5$ ) sorted by short-term net-directional connectedness extracted from aggregate (Panel A) and causal (Panel B) linkages. Each panel also reports correlations of principal components with a long-short network portfolio ( $\mathcal{N}(S)$ ) and benchmark strategies - dollar (dol), carry trade (car), volatility (vol), volatility risk premium (vrp), and momentum (mom). The sample is from January 1996 to December 2013.

<b>Panel A: Aggregate linkages</b>												
	PC loadings						Correlations					
	$\mathcal{P}_1$	$\mathcal{P}_2$	$\mathcal{P}_3$	$\mathcal{P}_4$	$\mathcal{P}_5$	CV	$\mathcal{N}(S)$	dol	car	vol	vrp	mom
PC1	0.53	0.52	0.44	0.38	0.32	76.03	-0.46	1.00	0.30	0.59	-0.05	0.00
PC2	-0.49	-0.43	0.35	0.60	0.32	84.34	0.58	0.05	0.47	0.19	-0.25	-0.01
PC3	-0.05	-0.04	-0.13	-0.46	0.87	90.85	0.59	0.04	0.06	0.07	-0.09	0.22
PC4	-0.10	-0.09	0.82	-0.53	-0.17	96.30	-0.04	-0.01	-0.07	0.15	-0.15	-0.07
PC5	-0.68	0.73	-0.02	-0.01	-0.02	100.00	0.32	-0.01	0.07	-0.07	-0.08	0.04

<b>Panel B: Causal linkages</b>												
	PC loadings						Correlations					
	$\mathcal{P}_1$	$\mathcal{P}_2$	$\mathcal{P}_3$	$\mathcal{P}_4$	$\mathcal{P}_5$	CV	$\mathcal{N}(S)$	dol	car	vol	vrp	mom
PC1	0.45	0.50	0.47	0.47	0.34	77.62	-0.26	1.00	0.32	0.60	-0.06	0.01
PC2	0.88	-0.15	-0.20	-0.36	-0.17	86.16	-0.79	0.01	0.18	0.06	-0.20	-0.06
PC3	0.07	-0.47	-0.32	0.18	0.80	92.08	0.46	0.04	0.31	0.11	-0.21	0.13
PC4	0.13	-0.42	-0.10	0.76	-0.47	96.27	-0.31	-0.01	0.01	0.00	-0.06	-0.01
PC5	0.01	-0.58	0.79	-0.20	0.02	100.00	0.01	0.00	-0.10	0.09	0.09	-0.12

ear models for the test excess returns sorted on causal connectedness. In particular, the two-factor SDFs has dol as the first factor plus a second factor, including car, vol, vrp, mom, or  $\mathcal{N}(S)$  one at a time. For the three-factor SDFs, we start with the two factors, dol and  $\mathcal{N}(S)$ , and then consider various third factors, including car, vol, vrp, or mom.

Table 13 presents the asset pricing results for all models considered, with Panel A showing the specifications in (A1), and Panels B and C reporting the frameworks in (A2). The results in Panel A indicate that none of the SDF loadings and risk prices for benchmark risk factors are statistically significant at the 5% level. In contrast, we document the positive and statistically significant loading (a t-stat of 2.38) and price (a t-stat of 2.15) of the network risk factor. In particular, the GMM estimate of  $\lambda_{\mathcal{N}(S)}$  is 0.47% per month. Since the network factor is actually tradable, we can apply the Euler equation to the factor excess returns and derive that its price of risk must be equal to the average excess return. Using statistics reported in Table 1, we verify that this no-arbitrage condition indeed holds: the monthly average return of 0.46% is close to the estimated price of 0.47%. Regarding the dollar factor, its SDF loading and price of risk are insignificant at conventional confidence levels

(a t-stat of 1.21 for  $b_{\text{dol}}$  and a t-stat of 0.66 for  $\lambda_{\text{dol}}$ ). Moreover, the estimated  $\lambda_{\text{dol}}$  matches the factor's average excess return of 0.13% per month, as reported in Table 3. Even though the dollar factor does not help to explain the average excess returns, it serves as a constant capturing the common mispricing in the cross-sectional regression.

In terms of the model fit, the two-factor SDFs combining the dollar and other benchmark risk factors produce similar performances, capturing from 32.61% to 47.06% of total variance in the cross-sectional returns and yielding RMSEs from 0.11% to 0.14%. We also cannot reject any of these linear models based on  $\text{HJ}_{\text{dist}}$  because the simulated p-values are far above 50% in all cases. At the same time, the SDF specification comprising the dollar and network risk factors outperforms other models by a large margin. For instance, it generates more than twice-as-large cross-sectional  $R^2$  of 97.18% and more than three times smaller RMSE and  $\text{HJ}_{\text{dist}}$  of 0.03% and 0.05.

In sum, the benchmark risk factors from the existing literature have a hard time explaining the network-sorted portfolios, whereas the network risk factor successfully prices the novel cross-section of currency returns documented in our paper. Furthermore, the quantitative results show a significant wedge in the contribution of the network and other factors, despite possible common components in their returns originating from the interest rate predictability (for car), contemporaneous correlations in spot variances (for vol) or spot implied variances (for vrp).

Panel B in Table 13 shows the results for portfolios sorted on the causal network measure. As can be expected, once we eliminate the contemporaneous effects in the network, the performance of the SDFs with car, vol and vrp risk factors deteriorates significantly. The t-statistics of SDF loadings and factor prices become even smaller in absolute terms. Further, the  $R^2$  statistics drop dramatically to 4.90% and 1.79% with car and vol as a second factor or become negative -9.82% in the case of vrp. Interestingly, the performance of the linear model with dol and mom remains the same, though the evidence on priced momentum risk is weak. In contrast, the factor loading and price of network risk become statistically significant at the 1% level (a t-stat of 2.89 for  $b_{\mathcal{N}(S)}$  and a t-stat of 2.92 for  $\lambda_{\mathcal{N}(S)}$ ). The model with the network factor also displays stronger explanatory power as measured by higher  $R^2$  (40.72%) and generates the lower pricing errors as measured by

**Table 13. Pricing Short-term Net-directional Network Portfolios**

This table presents cross-sectional asset pricing results. We price quintile portfolios ( $\mathcal{P}_i : i = 1, \dots, 5$ ) sorted by short-term net-directional connectedness. In Panels A and B, we construct two-factor linear SDFs with the dollar (dol) factor plus a second factor, including carry trade (car), volatility (vol), volatility risk premium (vrp), momentum (mom), and short-term net-directional network ( $\mathcal{N}(S)$ ) factors. In Panel C, we construct three-factor linear SDFs with dol,  $\mathcal{N}(S)$  plus a third factor, including car, vol, vrp, and mom. Each panel reports one-step GMM estimates of factor loadings ( $b$ ) and prices of factor risks ( $\lambda$ ). Goodness-of-fit statistics include the  $R^2$  and root mean squared pricing error (RMSE) (both are expressed in percentage), and the Hansen and Jagannathan (1997) distance ( $HJ_{\text{dist}}$ ) with simulated p-values in parentheses. The p-values are for the null hypothesis that pricing errors are equal to zero. The remaining numbers in rows with a grey font are t-statistics of estimates, which are based on Newey and West (1987) standard errors with Andrews (1991) optimal lag selection. The sample is from January 1996 to December 2013.

<b>Panel A: Aggregate linkages: two-factor models</b>									
	SDF loadings		Risk prices		Model fit				
	$b_{\text{dol}}$	$b_{f_2}$	$\lambda_{\text{dol}}$	$\lambda_{f_2}$	$R^2$ (%)	RMSE (%)	$HJ_{\text{dist}}$		
dol + car	-0.03	0.12	0.12	1.02	47.06	0.11	0.16		
	-0.55	1.73	0.50	1.78			(0.75)		
dol + vol	-0.14	0.25	0.12	1.12	23.00	0.14	0.21		
	-1.10	1.33	0.64	1.43			(0.58)		
dol + vrp	0.01	-0.25	0.12	-1.33	49.11	0.11	0.16		
	0.11	-1.46	0.48	-1.47			(0.78)		
dol + mom	0.02	0.26	0.12	1.94	32.61	0.13	0.16		
	0.35	1.57	0.40	1.57			(0.80)		
dol + $\mathcal{N}(S)$	0.07	0.10	0.13	0.47	97.18	0.03	0.05		
	1.55	2.38	0.66	2.15			(0.99)		
<b>Panel B: Causal linkages: two-factor models</b>									
dol + car	-0.03	0.12	0.12	1.00	4.90	0.20	0.32		
	-0.49	1.44	0.51	1.52			(0.42)		
dol + vol	-0.22	0.37	0.12	1.63	1.79	0.20	0.33		
	-0.96	1.07	0.62	1.12			(0.46)		
dol + vrp	0.02	-0.07	0.11	-0.40	-9.82	0.21	0.35		
	0.40	-0.67	0.55	-0.69			(0.29)		
dol + mom	0.02	0.43	0.12	3.19	32.04	0.17	0.30		
	0.25	1.94	0.31	1.94			(0.71)		
dol + $\mathcal{N}(S)$	0.04	0.09	0.12	0.43	40.72	0.16	0.25		
	1.21	2.89	0.66	2.92			(0.47)		
<b>Panel C: Causal linkages: three-factor models</b>									
	SDF loadings			Risk prices			Model fit		
	$b_{\text{dol}}$	$b_{f_2}$	$b_{\mathcal{N}(S)}$	$\lambda_{\text{dol}}$	$\lambda_{f_2}$	$\lambda_{\mathcal{N}(S)}$	$R^2$ (%)	RMSE (%)	$HJ_{\text{dist}}$
dol + car + $\mathcal{N}(S)$	-0.02	0.15	0.10	0.13	1.32	0.48	71.94	0.11	0.19
	-0.33	1.84	2.89	0.54	1.87	2.72			(0.69)
dol + vol + $\mathcal{N}(S)$	-0.01	0.18	0.10	0.12	0.85	0.45	56.81	0.13	0.22
	-0.41	0.64	2.58	0.70	0.70	2.58			(0.58)
dol + vrp + $\mathcal{N}(S)$	0.04	-0.23	0.11	0.13	-1.21	0.46	66.06	0.12	0.21
	0.83	-1.51	2.57	0.61	-1.49	2.37			(0.67)
dol + mom + $\mathcal{N}(S)$	0.03	0.19	0.06	0.12	1.49	0.44	45.45	0.15	0.25
	0.71	0.83	2.06	0.48	0.87	2.12			(0.58)

lower RMSE (0.16%) and  $HJ_{\text{dist}}$  (0.25).

In Panel C in Table 13, we extend the two-factor model with  $\text{dol}$  and  $\mathcal{N}(S)$  to the three-factor specification with  $\text{car}$ ,  $\text{vol}$ ,  $\text{vrp}$  or  $\text{mom}$ . The inclusion of an additional factor generally leads to higher  $R^2$ , lower RMSE and  $HJ_{\text{dist}}$  statistics relative to the original two-factor SDF. Most importantly, network risk remains strongly-priced in all specifications. Further, consistent with the principal component decomposition, the best-performing three-factor model includes the dollar, carry trade and network risk factors. Overall, the results emphasize the importance of network risk factors extracted from aggregate and especially causal currency connectedness in explaining the novel cross-sections of currency returns. These excess returns cannot be understood through the lens of benchmark factors.

#### 5.4 Time-series Exposure to Network Factors

We further estimate the sensitivity of excess returns of quintile portfolios ( $\mathcal{P}_i : i = 1, \dots, 5$ ) to the network risk. Table 14 reports the outputs of a contemporaneous regression of excess returns of each quintile portfolio on the dollar and network risk factors (Panel A) and on the dollar, carry trade/volatility, and network risk factors (Panel B).

For currency returns sorted on aggregate network connections, the estimated alphas are statistically insignificant. The  $\beta_{\text{dol}}$  coefficients are statistically indistinguishable from one. The  $\beta_{\text{net}}$  coefficients display a pronounced monotonicity when we move from  $\mathcal{P}_1$  to  $\mathcal{P}_5$ , increasing from -0.47 (a t-stat of -19.84) to 0.53 (a t-stat of 22.18). The two factors capture a lot of variation of quintile portfolios ranging from 67.35% for  $\mathcal{P}_4$  to 94.26% for  $\mathcal{P}_1$ .

For currency returns sorted on causal network connections, the right part of Panels A and Panel B reports the outputs for two- and three-factor regressions. The results suggest that the first, fourth and fifth portfolios have statistically significant alphas. The magnitude and the significance of alphas are generally reduced when we include additional risk factors, with the impact being particularly large for the inclusion of the carry trade. This can be explained by the observation that the exposure to the volatility factor is statistically insignificant for all portfolios, while the beta estimates for the carry trade are significant for three excess returns. The goodness of fit and slope coefficients of the network risk factor remain largely unchanged for two- and three-factor regressions.

Overall, the results of time-series regressions are consistent with cross-sectional regres-

**Table 14. Net-directional Network Portfolios: Factor Betas**

This table presents a contemporaneous regression of monthly excess returns of each quintile portfolio on two risk factors - the dollar and short-term net-directional network portfolios (Panel A), and on three risk factors - the dollar, carry/volatility, and short-term net-directional network portfolios (Panel B). Constants reported in the “alpha (% , annual)” row are expressed in percentage per annum. The numbers in rows with a grey font are t-statistics of estimates, which are based on [Newey and West \(1987\)](#) standard errors with [Andrews \(1991\)](#) optimal lag selection. The last row in each panel shows the adjusted  $R^2$  (in percentage). The sample is from January 1996 to December 2013.

<b>Panel A: Short-term net-directional portfolios</b>										
	Aggregate linkages					Causal linkages				
	$\mathcal{P}_1$	$\mathcal{P}_2$	$\mathcal{P}_3$	$\mathcal{P}_4$	$\mathcal{P}_5$	$\mathcal{P}_1$	$\mathcal{P}_2$	$\mathcal{P}_3$	$\mathcal{P}_4$	$\mathcal{P}_5$
alpha (% , annual)	0.34	-0.40	-0.13	-0.31	0.34	2.16	-1.03	-0.77	-2.74	2.16
	0.58	-0.32	-0.12	-0.21	0.58	3.11	-0.91	-0.76	-2.96	3.11
$\beta_{\text{dol}}$	0.99	1.09	1.01	0.91	0.99	0.88	1.11	1.05	1.08	0.88
	36.16	18.79	21.65	16.71	36.16	32.55	27.67	33.20	25.22	32.55
$\beta_{\mathcal{N}(s)}$	-0.47	-0.18	0.03	0.05	0.53	-0.57	0.00	0.03	0.13	0.43
	-19.84	-3.65	0.65	0.91	22.18	-15.34	0.07	0.91	3.37	11.39
$R^2(\%)$	94.26	83.70	75.81	67.35	89.51	91.66	82.70	82.06	81.92	86.37
<b>Panel B: Short-term net-directional portfolios: causal linkages</b>										
	car					vol				
	$\mathcal{P}_1$	$\mathcal{P}_2$	$\mathcal{P}_3$	$\mathcal{P}_4$	$\mathcal{P}_5$	$\mathcal{P}_1$	$\mathcal{P}_2$	$\mathcal{P}_3$	$\mathcal{P}_4$	$\mathcal{P}_5$
alpha (% , annual)	1.49	-0.48	0.02	-2.67	1.49	2.10	-0.91	-0.78	-2.72	2.10
	2.29	-0.42	0.02	-2.74	2.29	3.02	-0.81	-0.76	-2.91	3.02
$\beta_{\text{dol}}$	0.84	1.14	1.10	1.09	0.84	0.85	1.17	1.04	1.10	0.85
	28.44	27.04	31.17	24.51	28.44	22.04	22.56	24.04	20.79	22.04
$\beta_{f_2}$	0.10	-0.08	-0.12	-0.01	0.10	0.04	-0.09	0.01	-0.02	0.04
	3.27	-1.91	-3.79	-0.42	3.27	1.06	-1.72	0.11	-0.53	1.06
$\beta_{\mathcal{N}(s)}$	-0.57	0.00	0.03	0.13	0.43	-0.57	0.00	0.03	0.13	0.43
	-14.79	0.04	0.87	3.37	11.05	-15.72	0.05	0.91	3.36	11.69
$R^2(\%)$	92.67	83.37	83.64	81.93	88.02	91.75	83.15	82.06	81.95	86.52

sions. Specifically, they reinforce the conclusion that the dollar and network risk factors fully explain the sources of risk in the cross-section of aggregate or causal network portfolios, while the inclusion of the carry trade into a set of factors improves the representation of risks in causal connectedness portfolios.

## 6 Conclusion

We show that network risk among option-based variances on exchange rates predicts currency returns. A long-short portfolio strategy, which buys currencies receiving short-term shocks and sells currencies transmitting short-term shocks, generates a high Sharpe ratio and yields a significant alpha when controlling for popular foreign exchange benchmarks. Trading currency connectedness at longer horizons is less profitable, indicating a

downward-sloping term structure of network risk in currency markets. A network risk factor fully explains the cross-sectional variation of network-sorted excess returns, which cannot be understood through the lens of existing risk factors - dollar, carry trade, volatility, variance risk premium, and momentum. In robustness checks, we show that the performance of network portfolios in terms of risk-adjusted (Sharpe ratios) and benchmark adjusted (estimated alphas) performances actually improves when the strategies are implemented at daily or weekly frequencies. The significance of monthly network excess returns is also robust to transaction costs and subperiods.

Overall, the results of our paper provide new insights into the sources of currency predictability. We do not provide possible explanations for the returns and hence developing a formal theoretical model, which could rationalize our empirical findings, remains an open question. The common international linkages based on trade and cash-flow channels, which have been proposed to mainly explain the carry trade, are unlikely to capture the network returns, which remain uncorrelated with popular currency factors. We leave such an interesting and important avenue for future research.

## References

- Akram, Q. F., D. Rime, and L. Sarno (2008). Arbitrage in the foreign exchange market: Turning on the microscope. *Journal of International Economics* 76(2), 237–253.
- Andersen, L., D. Duffie, and Y. Song (2019). Funding value adjustments. *The Journal of Finance* 74(1), 145–192.
- Andrews, D. W. (1991). Heteroskedasticity and autocorrelation consistent covariance matrix estimation. *Econometrica: Journal of the Econometric Society*, 817–858.
- Asness, C. S., T. J. Moskowitz, and L. H. Pedersen (2013). Value and momentum everywhere. *The Journal of Finance* 68(3), 929–985.
- Bakshi, G., N. Kapadia, and D. Madan (2003). Stock return characteristics, skew laws, and the differential pricing of individual equity options. *The Review of Financial Studies* 16(1), 101–143.
- Bansal, R. and A. Yaron (2004). Risks for the long run: A potential resolution of asset pricing puzzles. *The Journal of Finance* 59 (4), 1481–1509.
- Barunik, J. and M. Ellington (2020). Dynamic networks in large financial and economic systems. *arXiv preprint arXiv:2007.07842*.
- BIS (2019a). Otc derivatives statistics at end-june 2019. *Bank for International Settlements, Basel*.
- BIS (2019b). Triennial central bank survey of foreign exchange and otc derivatives markets activity in 2019. *Bank for International Settlements, Basel*.
- Britten-Jones, M. and A. Neuberger (2000). Option prices, implied price processes, and stochastic volatility. *Journal of Finance* 55, 839–866.
- Burnside, C., M. Eichenbaum, I. Kleshchelski, and S. Rebelo (2011). Do peso problems explain the returns to the carry trade? *The Review of Financial Studies* 24(3), 853–891.
- Cespa, G., A. Gargano, S. J. Riddiough, and L. Sarno (2019). Foreign exchange volume. *Unpublished working paper. City University London, University of Cambridge, and The University of Melbourne*.
- Chernov, M., J. Graveline, and I. Zviadadze (2018). Crash risk in currency returns. *Journal of Financial and Quantitative Analysis* 53(1), 137–170.
- Cochrane, J. H. (2005). *Asset pricing*. Princeton university press.
- Colacito, R., M. M. Croce, F. Gavazzoni, and R. Ready (2018). Currency risk factors in a



- recursive multicountry economy. *The Journal of Finance* 73(6), 2719–2756.
- Colacito, R., S. J. Riddiough, and L. Sarno (2020). Business cycles and currency returns. *Journal of Financial Economics*.
- Corte, P. D., S. J. Riddiough, and L. Sarno (2016). Currency premia and global imbalances. *The Review of Financial Studies* 29(8), 2161–2193.
- Dahlhaus, R. (1996). On the kullback-leibler information divergence of locally stationary processes. *Stochastic processes and their applications* 62(1), 139–168.
- Dahlhaus, R., W. Polonik, et al. (2009). Empirical spectral processes for locally stationary time series. *Bernoulli* 15(1), 1–39.
- Dahlquist, M. and H. Hasseltoft (2020). Economic momentum and currency returns. *Journal of Financial Economics* 136(1), 152–167.
- Della Corte, P., R. Kozhan, and A. Neuberger (2020). The cross-section of currency volatility premia. *Journal of Financial Economics*.
- Della Corte, P., T. Ramadorai, and L. Sarno (2016). Volatility risk premia and exchange rate predictability. *Journal of Financial Economics* 120(1), 21–40.
- Dew-Becker, I., S. Giglio, A. Le, and M. Rodriguez (2017). The price of variance risk. *Journal of Financial Economics* 123(2), 225–250.
- Diebold, F. X. and K. Yilmaz (2014). On the network topology of variance decompositions: Measuring the connectedness of financial firms. *Journal of Econometrics* 182(1), 119–134.
- Du, W., A. Tepper, and A. Verdelhan (2018). Deviations from covered interest rate parity. *The Journal of Finance* 73(3), 915–957.
- Elliott, M., B. Golub, and M. O. Jackson (2014). Financial networks and contagion. *American Economic Review* 104(10), 3115–53.
- Fan, Z., J. M. Londono, and X. Xiao (2021). Equity tail risk and currency risk premiums. *Journal of Financial Economics*.
- Farhi, E., S. P. Fraiburger, X. Gabaix, R. Ranciere, and A. Verdelhan (2015). Crash risk in currency markets. Technical report, New York University, New York, NY.
- Gabaix, X. and M. Maggiori (2015). International liquidity and exchange rate dynamics. *The Quarterly Journal of Economics* 130(3), 1369–1420.
- Garman, M. B. and S. W. Kohlhagen (1983). Foreign currency option values. *Journal of international Money and Finance* 2(3), 231–237.

- Gilmore, S. and F. Hayashi (2011). Emerging market currency excess returns. *American Economic Journal: Macroeconomics* 3(4), 85–111.
- Glasserman, P. and H. P. Young (2016). Contagion in financial networks. *Journal of Economic Literature* 54(3), 779–831.
- Goyal, A. and A. Saretto (2009). Cross-section of option returns and volatility. *Journal of Financial Economics* 94(2), 310–326.
- Hansen, L. P. (1982). Large sample properties of generalized method of moments estimators. *Econometrica: Journal of the Econometric Society*, 1029–1054.
- Hansen, L. P. and R. Jagannathan (1997). Assessing specification errors in stochastic discount factor models. *The Journal of Finance* 52(2), 557–590.
- Herskovic, B. (2018). Networks in production: Asset pricing implications. *The Journal of Finance* 73(4), 1785–1818.
- Herskovic, B., B. Kelly, H. Lustig, and S. Van Nieuwerburgh (2020). Firm volatility in granular networks. *Journal of Political Economy* 128(11), 4097–4162.
- Jagannathan, R. and Z. Wang (1996). The conditional capm and the cross-section of expected returns. *The Journal of finance* 51(1), 3–53.
- Jurek, J. W. (2014). Crash-neutral currency carry trades. *Journal of Financial Economics* 113(3), 325–347.
- Kadiyala, K. R. and S. Karlsson (1997). Numerical methods for estimation and inference in Bayesian VAR-models. *Journal of Applied Econometrics* 12(2), 99–132.
- Kan, R. and C. Robotti (2008). Specification tests of asset pricing models using excess returns. *Journal of Empirical Finance* 15(5), 816–838.
- Lustig, H., N. Roussanov, and A. Verdelhan (2011). Common risk factors in currency markets. *The Review of Financial Studies* 24(11), 3731–3777.
- Lustig, H. and A. Verdelhan (2007). The cross section of foreign currency risk premia and consumption growth risk. *American Economic Review* 97(1), 89–117.
- Lütkepohl, H. (2005). *New introduction to multiple time series analysis*. Springer Science & Business Media.
- Lyons, R. K. et al. (2001). *The microstructure approach to exchange rates*, Volume 333. Citeseer.
- Menkhoff, L., L. Sarno, M. Schmeling, and A. Schrimpf (2012a). Carry trades and global foreign exchange volatility. *The Journal of Finance* 67(2), 681–718.

- Menkhoff, L., L. Sarno, M. Schmeling, and A. Schrimpf (2012b). Currency momentum strategies. *Journal of Financial Economics* 106(3), 660–684.
- Menkhoff, L., L. Sarno, M. Schmeling, and A. Schrimpf (2017). Currency value. *The Review of Financial Studies* 30(2), 416–441.
- Mueller, P., A. Stathopoulos, and A. Vedolin (2017). International correlation risk. *Journal of Financial Economics* 126(2), 270–299.
- Newey, W. and K. West (1987). A simple, positive semi-definite, heteroskedasticity and autocorrelation consistent covariance matrix. *Econometrica*, 703–708.
- Pesaran, H. H. and Y. Shin (1998). Generalized impulse response analysis in linear multivariate models. *Economics letters* 58(1), 17–29.
- Petrova, K. (2019). A quasi-Bayesian local likelihood approach to time varying parameter VAR models. *Journal of Econometrics*.
- Rambachan, A. and N. Shephard (2019). Econometric analysis of potential outcomes time series: instruments, shocks, linearity and the causal response function. *arXiv preprint arXiv:1903.01637*.
- Richmond, R. J. (2019). Trade network centrality and currency risk premia. *The Journal of Finance* 74(3), 1315–1361.
- Zviadadze, I. (2017). Term structure of consumption risk premia in the cross section of currency returns. *The Journal of Finance* 72(4), 1529–1566.

# Appendix for “Currency Network Risk”

## Abstract

This appendix presents supplementary details not included in the main body of the paper.

## Contents

A. Estimation of the time-varying parameter VAR model	50
B. Asset Pricing Tests	52
C. Transaction Costs	54

## A Estimation of the time-varying parameter VAR model

Let  $\mathbf{CIV}_t$  be an  $N \times 1$  vector generated by a stable time-varying parameter (TVP) heteroskedastic VAR model with  $p$  lags:

$$\mathbf{CIV}_{t,T} = \Phi_1(t/T)\mathbf{CIV}_{t-1,T} + \dots + \Phi_p(t/T)\mathbf{CIV}_{t-p,T} + \epsilon_{t,T}, \quad (\text{A.1})$$

where  $\epsilon_{t,T} = \Sigma^{-1/2}(t/T)\eta_{t,T}$ ,  $\eta_{t,T} \sim NID(0, \mathbf{I}_M)$  and  $\Phi(t/T) = (\Phi_1(t/T), \dots, \Phi_p(t/T))^\top$  are the time varying autoregressive coefficients. Note that all roots of the polynomial  $\chi(z) = \det(\mathbf{I}_N - \sum_{p=1}^L z^p \mathbf{B}_{p,t})$  lie outside the unit circle, and  $\Sigma_t^{-1}$  is a positive definite time-varying covariance matrix. Stacking the time-varying intercepts and autoregressive matrices in the vector  $\phi_{t,T}$  with  $\overline{\mathbf{CIV}}_t^\top = (\mathbf{I}_N \otimes x_t)$ ,  $x_t = (1, x_{t-1}^\top, \dots, x_{t-p}^\top)$  and denoting the Kronecker product by  $\otimes$ , the model can be written as:

$$\mathbf{CIV}_{t,T} = \overline{\mathbf{CIV}}_{t,T}^\top \phi_{t,T} + \Sigma_{t/T}^{-\frac{1}{2}} \eta_{t,T} \quad (\text{A.2})$$

We obtain the time-varying parameters of the model by employing the Quasi-Bayesian Local-Likelihood (QBLL) approach of Petrova (2019). The estimation of Eq. (A.1) requires re-weighting the likelihood function. The weighting function gives higher proportions to observations surrounding the time period whose parameter values are of interest. The local likelihood function at time period  $k$  is given by:

$$\begin{aligned} L_k(\mathbf{CIV} | \theta_k, \Sigma_k, \overline{\mathbf{CIV}}) &\propto \\ &|\Sigma_k|^{\text{trace}(\mathbf{D}_k)/2} \exp \left\{ -\frac{1}{2} (\mathbf{CIV} - \overline{\mathbf{CIV}}^\top \phi_k)^\top (\Sigma_k \otimes \mathbf{D}_k) (\mathbf{CIV} - \overline{\mathbf{CIV}}^\top \phi_k) \right\} \end{aligned} \quad (\text{A.3})$$

$\mathbf{D}_k$  is a diagonal matrix whose elements hold the weights:

$$\mathbf{D}_k = \text{diag}(q_{k1}, \dots, q_{kT}) \quad (\text{A.4})$$

$$q_{kt} = \phi_{T,k} w_{kt} / \sum_{t=1}^T w_{kt} \quad (\text{A.5})$$

$$w_{kt} = (1/\sqrt{2\pi}) \exp((-1/2)((k-t)/H)^2), \quad \text{for } k, t \in \{1, \dots, T\} \quad (\text{A.6})$$

$$\zeta_{Tk} = \left( \left( \sum_{t=1}^T w_{kt} \right)^2 \right)^{-1} \quad (\text{A.7})$$

where  $q_{kt}$  is a normalised kernel function.  $w_{kt}$  uses a Normal kernel weighting function.

$\zeta_{Tk}$  gives the rate of convergence and behaves like the bandwidth parameter  $H$  in (A.6). The kernel function puts a greater weight on the observations surrounding the parameter estimates at time  $k$  relative to more distant observations.

We use a Normal-Wishart prior distribution for  $\phi_k | \Sigma_k$  for  $k \in \{1, \dots, T\}$ :

$$\phi_k | \Sigma_k \sim \mathcal{N} \left( \phi_{0k}, (\Sigma_k \otimes \Xi_{0k})^{-1} \right) \quad (\text{A.8})$$

$$\Sigma_k \sim \mathcal{W} (\alpha_{0k}, \Gamma_{0k}) \quad (\text{A.9})$$

where  $\phi_{0k}$  is a vector of prior means,  $\Xi_{0k}$  is a positive definite matrix,  $\alpha_{0k}$  is a scale parameter of the Wishart distribution ( $\mathcal{W}$ ), and  $\Gamma_{0k}$  is a positive definite matrix.

The prior and weighted likelihood function implies a Normal-Wishart quasi posterior distribution for  $\phi_k | \Sigma_k$  for  $k = \{1, \dots, T\}$ . Formally, let  $\mathbf{A} = (\bar{x}_1^\top, \dots, \bar{x}_T^\top)^\top$  and  $\mathbf{Y} = (x_1, \dots, x_T)^\top$ , then:

$$\phi_k | \Sigma_k, \mathbf{A}, \mathbf{Y} \sim \mathcal{N} \left( \tilde{\theta}_k, (\Sigma_k \otimes \tilde{\Xi}_k)^{-1} \right) \quad (\text{A.10})$$

$$\Sigma_k \sim \mathcal{W} (\tilde{\alpha}_k, \tilde{\Gamma}_k^{-1}) \quad (\text{A.11})$$

with quasi posterior parameters

$$\tilde{\phi}_k = \left( \mathbf{I}_N \otimes \tilde{\Xi}_k^{-1} \right) \left[ \left( \mathbf{I}_N \otimes \mathbf{A}^\top \mathbf{D}_k \mathbf{A} \right) \hat{\phi}_k + \left( \mathbf{I}_N \otimes \Xi_{0k} \right) \phi_{0k} \right] \quad (\text{A.12})$$

$$\tilde{\Xi}_k = \Xi_{0k} + \mathbf{A}^\top \mathbf{D}_k \mathbf{A} \quad (\text{A.13})$$

$$\tilde{\alpha}_k = \alpha_{0k} + \sum_{t=1}^T q_{kt} \quad (\text{A.14})$$

$$\tilde{\Gamma}_k = \Gamma_{0k} + \mathbf{Y}' \mathbf{D}_k \mathbf{Y} + \Phi_{0k} \Gamma_{0k} \Phi_{0k}^\top - \tilde{\Phi}_k \tilde{\Gamma}_k \tilde{\Phi}_k^\top \quad (\text{A.15})$$

where  $\hat{\phi}_k = (\mathbf{I}_N \otimes \mathbf{A}^\top \mathbf{D}_k \mathbf{A})^{-1} (\mathbf{I}_N \otimes \mathbf{A}^\top \mathbf{D}_k) \mathbf{y}$  is the local likelihood estimator for  $\phi_k$ . The matrices  $\Phi_{0k}$ ,  $\tilde{\Phi}_k$  are conformable matrices from the vector of prior means,  $\phi_{0k}$ , and a draw from the quasi posterior distribution,  $\tilde{\phi}_k$ , respectively.

The motivation for employing these methods are threefold. First, we are able to estimate large systems that conventional Bayesian estimation methods do not permit. This is typically because the state-space representation of an  $N$ -dimensional TVP VAR ( $p$ ) requires an additional  $N(3/2 + N(p + 1/2))$  state equations for every additional variable. Conventional Markov Chain Monte Carlo (MCMC) methods fail to estimate larger models, which



in general confine one to (usually) fewer than 6 variables in the system. Second, the standard approach is fully parametric and requires a law of motion. This can distort inference if the true law of motion is misspecified. Third, the methods used here permit direct estimation of the VAR's time-varying covariance matrix, which has an inverse-Wishart density and is symmetric positive definite at every point in time.

In estimating the model, we use  $p=2$  and a Minnesota Normal-Wishart prior with a shrinkage value  $\varphi = 0.05$  and centre the coefficient on the first lag of each variable to 0.1 in each respective equation. The prior for the Wishart parameters are set following [Kadiyala and Karlsson \(1997\)](#). For each point in time, we run 500 simulations of the model to generate the (quasi) posterior distribution of parameter estimates. Note we experiment with various lag lengths,  $p = \{2, 3, 4, 5\}$ ; shrinkage values,  $\varphi = \{0.01, 0.25, 0.5\}$ ; and values to centre the coefficient on the first lag of each variable,  $\{0, 0.05, 0.2, 0.5\}$ . Network measures from these experiments are qualitatively similar. Notably, adding lags to the VAR and increasing the persistence in the prior value of the first lagged dependent variable in each equation increases computation time.

## B Asset Pricing Tests

The standard Euler equation implies that the excess returns  $rx_{t+1}^j$  of a portfolio  $j$  satisfy the equation:

$$\mathbb{E}_t \left( M_{t+1} rx_{t+1}^j \right) = 0, \quad (\text{B.16})$$

in which  $M_{t+1}$  is the stochastic discount factor (SDF). We assume that the SDF is a linear function of a set of risk factors  $f_{t+1}$  and is defined as follows:

$$M_{t+1} = 1 - b'(f_{t+1} - \mu_f). \quad (\text{B.17})$$

Notice that we employ a de-meanned version of the SDF to avoid the issue related to an affine transformation of factors ([Kan and Robotti, 2008](#)).

We are interested in testing the performance of linear pricing models defined by Eq. (B.16)-(B.17). To do so, we estimate factor loadings using the generalized method of moments (GMM) ([Hansen, 1982](#)). Substituting Eq. (B.17) into Eq. (B.16), we obtain the following  $N$  moment conditions  $\mathbb{E}_t \left( [1 - b'(f_{t+1} - \mu_f)] rx_{t+1} \right) = 0_N$ , where  $rx_{t+1}$  is the  $N$ -

dimensional vector of test asset excess returns. We simultaneously estimate the unknown vector of factor means  $\mu_f$ . Thus, GMM moment conditions also include the set of  $k$  restrictions  $\mathbb{E}_t (f_{t+1} - \mu_f) = 0_k$ , where  $k$  denotes the number of factors in the SDF specification. Therefore, we have the following population moment conditions:

$$\mathbb{E}_t [g_{t+1}(\theta)] = \mathbb{E}_t \begin{bmatrix} [1 - b'(f_{t+1} - \mu_f)]rx_{t+1} \\ f_{t+1} - \mu_f \end{bmatrix} = 0_{N+k},$$

where  $\theta = (b', \mu_f)'$  is the vector of parameters. The sample moment conditions are then defined as:

$$\bar{g}_T(\theta) = \begin{bmatrix} \bar{g}_T^1(\theta) \\ \bar{g}_T^2(\theta) \end{bmatrix} = \begin{bmatrix} \frac{1}{T} \sum_{t=1}^T [1 - b'(f_{t+1} - \mu_f)] rx_{t+1} \\ \frac{1}{T} \sum_{t=1}^T [f_{t+1} - \mu_f] \end{bmatrix}.$$

We implement a one-stage GMM estimation with the prespecified weighting matrix consisting of the identity matrix  $I_N$  for the first moment conditions and a large weight assigned to the remaining restrictions. Standard errors are computed based on a heteroscedasticity and autocorrelation consistent (HAC) estimate of the long-run covariance matrix  $S = \sum_{j=-\infty}^{\infty} \mathbb{E}[g(\theta)g(\theta)']$  by the [Newey and West \(1987\)](#) procedure with [Andrews \(1991\)](#) optimal lag selection.

We now evaluate the performance of linear pricing models in explaining the cross-section of network portfolios. We construct the cross-sectional  $R^2$ , root mean squared pricing error (RMSE), and the [Hansen and Jagannathan \(1997\)](#) distance ( $\text{HJ}_{\text{dist}}$ ). [Hansen and Jagannathan \(1997\)](#) provide two nice illustrations of  $\text{HJ}_{\text{dist}}$ . First, it is the maximum pricing error of a portfolio with a unit second moment. Second, it measures the minimum distance between the proposed SDF and the set of admissible SDFs. Thus, tests of linear SDFs defined by Eq. (B.17) boil down to testing the null hypothesis that the pricing errors equal zero, i.e.  $\text{HJ}_{\text{dist}}$  equals zero. Formally, the [Hansen and Jagannathan \(1997\)](#) distance is defined as:

$$\text{HJ}_{\text{dist}} = \sqrt{\min_{\theta} \bar{g}_T(\theta)' G_T^{-1} \bar{g}_T(\theta)}, \quad (\text{B.18})$$

in which  $G_T$  is the sample second moment matrix of test excess returns, that is,  $G_T = \frac{1}{T} \sum_{t=1}^T rx_{t+1}rx'_{t+1}$ . One can obtain  $\text{HJ}_{\text{dist}}$  by applying the one-stage GMM estimation with the weighting matrix equal to  $G_T^{-1}$ . The advantage of this definition is that  $G_T^{-1}$  is indepen-

dent of optimal parameters and hence this allows the comparison between different SDF specifications (Hansen and Jagannathan, 1997). The disadvantage of this approach is that  $G_T^{-1}$  is not optimal in the sense of Hansen (1982) and hence  $HJ_{\text{dist}}$  is not asymptotically a random variable of  $\chi^2(N - k)$  distribution. Instead, the sample  $HJ_{\text{dist}}$  follows a weighted sum of  $\chi^2(1)$  random variables (see Jagannathan and Wang (1996) and Kan and Robotti (2008) for specification tests using gross and excess returns, respectively). Therefore, we calculate the simulated p-values for  $HJ_{\text{dist}}$  based on this statistic.

## C Transaction Costs

We use time-varying quoted bid-ask spreads to compute the currency excess returns adjusted for transaction costs. Following Menkhoff et al. (2012b), we take into account the whole cycle of each currency in the short or long positions from  $t - 1$  to  $t + 1$ . When the investor buys the currency at time  $t$  and sells at time  $t + 1$ , he pays the corresponding bid-ask costs each period. In our notations, the excess returns of long ( $l$ ) and short ( $s$ ) positions are respectively  $rx_{t+1}^l = f_t^b - s_{t+1}^a$  and  $rx_{t+1}^s = -f_t^a + s_{t+1}^b$ . If the investor buys the currency at time  $t$  but decides to keep it in the portfolio at time  $t + 1$ , then the net excess returns are computed as  $rx_{t+1}^l = f_t^b - s_{t+1}$  and  $rx_{t+1}^s = -f_t^a + s_{t+1}$ . If the currency, which belongs to the portfolio at time  $t$  and is sold at time  $t + 1$ , was already in the current portfolio at time  $t - 1$ , then the excess returns  $rx_{t+1}^l = f_t^b - s_{t+1}^a$  and  $rx_{t+1}^s = -f_t^a + s_{t+1}^b$ , that is, the investor must still initiate a position in the one-month forward contract. At the start (January 1996) and at the end (December 2013) of the sample, the investor is assumed to start and close positions in all foreign currencies.